SIAM J. APPL. MATH.
Vol. 64, No. 1, pp. 41–80

STRONGLY DEGENERATE PARABOLIC-HYPERBOLIC SYSTEMS MODELING POLYDISPERSE SEDIMENTATION WITH COMPRESSION*

STEFAN BERRES†, RAIMUND BÜRGER†, KENNETH H. KARLSEN‡, AND ELMER M. TORY§

Abstract. We show how existing models for the sedimentation of monodisperse flocculated suspensions and of polydisperse suspensions of rigid spheres differing in size can be combined to yield a new theory of the sedimentation processes of polydisperse suspensions forming compressible sediments ("sedimentation with compression" or "sedimentation-consolidation process"). For N solid particle species, this theory reduces in one space dimension to an $N \times N$ coupled system of quasi-linear degenerate convection-diffusion equations. Analyses of the characteristic polynomials of the Jacobian of the convective flux vector and of the diffusion matrix show that this system is of strongly degenerate parabolic-hyperbolic type for arbitrary N and particle size distributions. Bounds for the eigenvalues of both matrices are derived. The mathematical model for $N = 3$ is illustrated by a numerical simulation obtained by the Kurganov–Tadmor central difference scheme for convection-diffusion problems. The numerical scheme exploits the derived bounds on the eigenvalues to keep the numerical diffusion to a minimum.

Key words. polydisperse suspensions, sedimentation, systems of conservation laws, strongly degenerate parabolic-hyperbolic systems, central difference approximation

AMS subject classifications. 35K65, 35L40, 35L65, 65M06, 76T05

DOI. 10.1137/S0036139902408163

1. Introduction.

Mathematical models for the (controlled) sedimentation of polydisperse suspensions of small particles, which belong to a finite number of species differing in size or density and are suspended in a viscous fluid, are important to many applications such as the chemical engineering, ceramic, pulp and paper, and food industries, mineral processing, wastewater treatment, and medicine [3, 50, 88, 89, 101, 122]. The characteristic behavior of such mixtures is differential sedimentation, which leads to areas of different composition if an initially homogeneous suspension is allowed to settle. In this paper, we consider the additional property that the solid particles possibly form a compressible sediment layer. A mathematical model for polydisperse suspensions forming compressible sediments is developed, analyzed, and simulated, focusing on three different aspects.

First, we show how two existing sedimentation models—one for monodisperse flocculated suspensions, which are described by *scalar* strongly degenerate parabolic-hyperbolic equations, and one for polydisperse suspensions of rigid spheres differing

*Received by the editors May 20, 2002; accepted for publication (in revised form) March 24, 2003; published electronically October 14, 2003. This work was supported (in part) by the Sonderforschungsbereich 404 at the University of Stuttgart, by the BeMatA program of the Research Council of Norway, and by the European network HYKE, funded by the EC as contract HPRN-CT-2002-00282.

http://www.siam.org/journals/siap/64-1/40816.html

†Institute of Applied Analysis and Numerical Simulation, University of Stuttgart, Pfaffenwaldring 57, D-70569 Stuttgart, Germany (berres@mathematik.uni-stuttgart.de, buerger@mathematik.uni-stuttgart.de).

‡Department of Mathematics, University of Bergen, Johs. Brunsgt. 12, N-5008 Bergen, Norway, and Centre of Mathematics for Applications, Department of Mathematics, University of Oslo, P.O. Box 1053, Blindern, N-0316 Oslo, Norway (kennethk@mi.uib.no).

§Department of Mathematics and Computer Science (Emeritus), Mount Allison University, Sackville, NB, E4L 1E8 Canada (sherpa@nbnet.nb.ca).

in size, which lead to *first-order systems* of conservation laws—can be combined into a model of sedimentation of polydisperse suspensions of particles (or flocs) forming compressible sediments.

Secondly, we prove that this model gives rise to strongly degenerate parabolic-hyperbolic systems of PDEs. (A precise definition of that type property is given below.) This type characterization is valid for arbitrary numbers N of sizes of equal-density particles. The application considered thus provides provably strongly degenerate parabolic-hyperbolic systems of arbitrary size. The well-posedness analysis and design of numerical schemes for such equations has received considerable interest in recent years, but, especially in the system (nonscalar) case, only a few applications are known. The present paper provides such an application.

Finally, for $N = 3$ we illustrate the model by numerical examples using the high-resolution Kurganov–Tadmor central difference scheme [64]. Its exposition in [64] is biased towards systems of conservation laws but also suggests an extension to parabolic-hyperbolic systems. This paper presents the first (to our knowledge) application of that extension to a realistic model.

In what follows, we outline the paper and put it in perspective relative to the existing literature. In section 2, we derive a set of spatially multidimensional model equations for the sedimentation of polydisperse suspensions forming compressible sediments (also called a sedimentation-consolidation process). The modeling starts from the usual mass and linear momentum balance equations for the N solids species (each regarded as one phase) and the fluid. The generic material properties of the suspension are introduced by constitutive assumptions concerning the solid and fluid stress tensors and the solid-fluid interaction forces. In particular, the solid phase pressures and the fluid pressure are replaced by the effective solid stress σ_e and the pore pressure. Here we assume that σ_e is a function of the total solids concentration $\phi := \phi_1 + \cdots + \phi_N$ only, where ϕ_i is the concentration of species i having diameter d_i and density ϱ_i. The way in which σ_e depends on ϕ_1 to ϕ_N determines the resulting diffusion matrix of the above-mentioned degenerate system. Specifying the solid-fluid interaction force for each species and finally performing a dimensional analysis, which permits our neglecting several terms of the linear momentum balance equations, we obtain explicit expressions for the solid-fluid relative velocity (or slip velocity) of each species as a function of $\Phi := (\phi_1, \ldots, \phi_N)^{\mathrm{T}}$ and $\nabla\Phi$, which in turn yield the fluxes of the continuity equations. The final (spatially multidimensional) model equations form a strongly degenerate system of N convection-diffusion equations for $\phi_1, \ldots, \phi_N$ coupled to the divergence-free condition of the volume-average mixture velocity and a three-component equation for the motion of the mixture. These last two equations account for viscous effects and reduce for $\Phi \equiv 0$ to the Stokes system for an incompressible fluid. Finally, we check that for $N = 1$ the strongly degenerate system reduces to the known scalar equation for monodisperse suspensions [26]. An overview of the analysis, numerics, and applications of strongly degenerate parabolic equations is given in section 5. For incompressible sediments, i.e., when $\sigma_e \equiv 0$, the model reduces to the Masliyah–Lockett–Bassoon (MLB) model [71, 73] for polydisperse suspensions of rigid spheres.

The effect of compressible sediment in polydisperse sedimentation has been studied only infrequently [98, 102]. Unfortunately, these treatments are incomplete in that they are not embedded in the appropriate mathematical PDE framework or are limited to $N = 2$. We assume that the mixture forms a compressible sediment layer whenever the cumulative solids concentration ϕ exceeds a critical value (or "gel

point") ϕ_c, and is in hindered settling for $\phi \le \phi_c$. In [102], however, the transition between the hindered settling zone (where $\phi \le \phi_c$) and the compression region (where $\phi > \phi_c$) is introduced by an artificial moving boundary condition, which we avoid by the concept of a degenerate diffusion equation. Our model also describes the relative movement of the solids species against each other within the sediment under the influence of the effective solid stress. This is unlike any previous treatment. Thus, our model is new and therefore derived completely in section 2. On the other hand, we essentially combine arguments that have been discussed extensively in previous works that focus on modeling either flocculated monodisperse [26, 27, 35] or nonflocculated polydisperse suspensions [14, 19, 22]. Thus the presentation in section 2 is fairly concise, and we refer to the cited papers for additional details and justification.

To continue the discussion, we need a precise definition of strongly degenerate parabolic-hyperbolic systems. In fact, in recent years we have seen an increased interest in quasi-linear systems of PDEs that in one space dimension can be written as

$$\frac{\partial \mathbf{u}}{\partial t} + \frac{\partial \boldsymbol{\varphi}(\mathbf{u})}{\partial x} = \frac{\partial}{\partial x}\left(\mathbf{D}(\mathbf{u})\frac{\partial \mathbf{u}}{\partial x}\right), \quad x \in \mathbb{R},\ t > 0, \tag{1.1}$$

where $\mathbf{u} : \mathbb{R} \times \mathbb{R}^+ \to \mathcal{D} \subset \mathbb{R}^N$ is the sought solution vector, $\boldsymbol{\varphi} : \mathcal{D} \to \mathbb{R}^N$ is a flux vector, and $\mathbf{D} : \mathcal{D} \to \mathbb{R}^{N\times N}$ is a diffusion matrix. We allow the system to be degenerate in the sense that $\mathbf{D}(\mathbf{u}) = 0$ for $\mathbf{u} \in \mathcal{D}' \subset \mathcal{D}$; i.e., the system reduces to first order on $\mathcal{D}'$. The system is called *strongly degenerate* if $\mathcal{D}'$ is of nonzero N-dimensional measure. Moreover, we recall that the system (1.1) is *strictly parabolic* at a point $\mathbf{u}_0 \in \mathcal{D}$ if $\mathbf{D}(\mathbf{u}_0) > 0$; i.e., the matrix $\mathbf{D}(\mathbf{u}_0)$ has only positive eigenvalues. On the other hand, if $\mathbf{u}_0$ is chosen such that $\mathbf{D}(\mathbf{u}_0) = 0$, then, according to the usual terminology for conservation laws, the system (1.1) is called *hyperbolic* if the Jacobian $\boldsymbol{\mathcal{J}}_{\boldsymbol{\varphi}}(\mathbf{u}_0)$ has N real eigenvalues, and *strictly hyperbolic* if these eigenvalues are moreover pairwise distinct. Finally, we shall call (1.1) a *strongly degenerate parabolic-hyperbolic system* if, at any point $\mathbf{u}_0$ belonging to the interior $\mathcal{D}^0$ of $\mathcal{D}$, the system (1.1) is either strictly parabolic or strictly hyperbolic in the sense given above and the set $\mathcal{D}^0 \cap \mathcal{D}'$ on which the system is strictly hyperbolic is of nonzero N-dimensional measure. We emphasize here that points $\mathbf{u} \in \mathcal{D}\backslash\mathcal{D}^0$, which are on the boundary of the physically relevant region $\mathcal{D}$, do not enter the type characterization [59]. Note that a strictly hyperbolic first-order system of conservation laws, for which the right-hand side of (1.1) vanishes identically, is included as a special case. Of course, solutions of (1.1) are in general discontinuous, even for smooth initial data. Further properties are discussed in section 5.

If the multidimensional sedimentation equations developed in section 2 are restricted to one space dimension, the motion of the mixture is determined by the velocity at one end of the computational domain. For a closed vessel, this velocity is zero, and only the degenerate system for $\phi_1, \ldots, \phi_N$ needs to be solved. This system of second-order PDEs can then be written as

$$\frac{\partial \Phi}{\partial t} + \frac{\partial \mathbf{f}(\Phi)}{\partial z} = \frac{\partial}{\partial z}\left(\mathbf{A}(\Phi)\frac{\partial \Phi}{\partial z}\right), \tag{1.2}$$

where t is time and z is height. In section 2, we assume that $\sigma_e = 0$ for $\phi \le \phi_c$. This assumption implies $\mathbf{A}(\Phi) = 0$ for $\phi \le \phi_c$. In this case, the system (1.2) is reduced to the first-order system

$$\frac{\partial \Phi}{\partial t} + \frac{\partial \mathbf{f}(\Phi)}{\partial z} = 0. \tag{1.3}$$

We consider the system (1.2) for vectors $\Phi \in \mathcal{D}_{\phi_{\max}}$, where $0 < \phi_{\max} \leq 1$ denotes the maximum admissible cumulative solids concentration, and we define for $0 < \phi_{\mathrm{M}} \leq 1$

$$\mathcal{D}_{\phi_{\mathrm{M}}} := \big\{\Phi = (\phi_1, \ldots, \phi_N) \in \mathbb{R}^N : \phi_1 \geq 0, \ldots, \phi_N \geq 0;\ \phi_1 + \cdots + \phi_N \leq \phi_{\mathrm{M}}\big\}.$$

Moreover, we denote by $\mathcal{D}^0_{\phi_{\mathrm{M}}}$ the interior of $\mathcal{D}_{\phi_{\mathrm{M}}}$, that is,

$$\mathcal{D}^0_{\phi_{\mathrm{M}}} := \big\{\Phi = (\phi_1, \ldots, \phi_N) \in \mathbb{R}^N : \phi_1 > 0, \ldots, \phi_N > 0;\ \phi_1 + \cdots + \phi_N < \phi_{\mathrm{M}}\big\}.$$

Obviously, the type of (1.2) is determined by the properties of $\mathbf{A}(\Phi)$ for $\phi_{\mathrm{c}} < \phi < \phi_{\max}$ and by those of the vector $\mathbf{f}(\Phi)$ (more precisely, of its Jacobian $\boldsymbol{\mathcal{J}}_{\mathbf{f}}(\Phi)$) for $0 < \phi \leq \phi_{\mathrm{c}}$ and $\phi = \phi_{\max}$. Since every component of $\mathbf{f}(\Phi) = (f_1(\Phi), \ldots, f_N(\Phi))^{\mathrm{T}}$ depends nonlinearly on every component of Φ, and since $\boldsymbol{\mathcal{J}}_{\mathbf{f}}(\Phi)$ is unsymmetric, it is by no means obvious that the system (1.3) is strictly hyperbolic. Since all entries of $\mathbf{A}(\Phi)$ are nonzero on $\mathcal{D}^0_{\phi_{\max}} \backslash \mathcal{D}_{\phi_{\mathrm{c}}}$, it is not apparent either that the system (1.2) is strictly parabolic for $\phi \in \mathcal{D}^0_{\phi_{\max}} \backslash \mathcal{D}_{\phi_{\mathrm{c}}}$. The core of this paper is formed by sections 3 and 4, where these properties are established by analyzing the characteristic polynomials of $\boldsymbol{\mathcal{J}}_{\mathbf{f}}(\Phi)$ and $\mathbf{A}(\Phi)$, respectively, where the vector $\mathbf{f}(\Phi)$ and the matrix $\mathbf{A}(\Phi)$ are chosen according to the model developed in section 2. Moreover, for the analysis of section 3, we assume that the particles all have the same density and that the species differ in size only. Our treatment has in part been inspired by Rosso and Sona's recent analysis of equations modeling the separation of oil-water dispersions [87]. In section 3, we discuss the properties of the system (1.3) with $\mathbf{f}(\Phi) = \mathbf{f}^{\mathrm{M}}(\Phi)$,

$$\frac{\partial \phi_i}{\partial t} + \frac{\partial f_i^{\mathrm{M}}(\Phi)}{\partial z} = 0, \quad i = 1, \ldots, N, \tag{1.4}$$

which arises from the model derived in section 2 by considering one space dimension and a closed settling vessel and assuming that the effective solid stress vanishes ($\sigma_{\mathrm{e}} \equiv 0$). The "M" indicates that the constitutive assumptions in section 2 have been chosen according to the MLB approach [22, 71, 73] (see [14, 22] for alternate equations for $\mathbf{f}(\Phi)$). The analysis of section 3 leads to the type of the system (1.2) for $\phi \leq \phi_{\mathrm{c}}$ and fully determines its type for $\sigma_{\mathrm{e}} \equiv 0$, that is, for a suspension of rigid particles [14, 19, 22]. The main result is that in the equal-density case, the system (1.4) is indeed strictly hyperbolic for all $\Phi \in \mathcal{D}^0_{\phi_{\max}}$ for $0 < \phi_{\max} \leq 1$. Strict hyperbolicity holds for all N and arbitrary particle sizes $d_1 > d_2 > \cdots > d_N > 0$.

To outline the significance of the analysis of section 3 in nontechnical terms, let us first say that hyperbolicity of a first-order system of conservation laws like (1.3) is in general a desirable property. In fact, the existence of a complete set of pairwise-distinct eigenvalues at each relevant point Φ of the state space ensures that the solution of (1.3) involves (simple) waves, i.e., solutions which essentially involve one eigenvalue of the Jacobian $\boldsymbol{\mathcal{J}}_{\mathbf{f}}(\Phi)$ and a corresponding eigenvector; see [51] for details. The important point is that each eigenvalue represents a finite propagation speed of solution information. For a mixture of flowing phases (in our case, the N "particulate" phases and the fluid), we should expect not only that a good model predicts finite speeds of propagation, but that moreover no solution information travels faster than any of the physical phases. We shall show later (Lemma 6.1 in section 6.3) that the MLB model for equal-density spheres and dilute to moderately concentrated suspensions indeed satisfies this requirement.

To put the hyperbolicity result in the proper perspective, let us now look at the opposite situation. Loss of hyperbolicity for a given vector $\Phi \in \mathbb{R}^N$ means that system

(1.4) has at least one pair of complex-conjugate eigenvalues. For $N = 2$, we then say that the system is *elliptic*. In most cases, for vectors Φ chosen from some subregion of the relevant state space, the system (1.4) is nonhyperbolic or elliptic and is hyperbolic elsewhere. Such systems are called *mixed systems*; see [47] for a survey of applications. In some applications, such as multiphase flow in porous media, the significance of mixed systems is essentially unclear, and loss of hyperbolicity is sometimes related to a model error. For polydisperse sedimentation, however, it is shown in [22] that for arbitrary N the degeneracy into nonhyperbolic type is a criterion for the possible occurrence of horizontal structures like fingers, columns, or blobs during sedimentation. This interpretation of nonhyperbolicity generalizes a criterion formulated in [4] for $N = 2$. Such instabilities have been observed in experiments [4, 117] at certain initial concentrations and are particularly likely to occur in suspensions including one species that is heavier and one that is lighter than the fluid. On the other hand, instabilities have never been observed with equal-density particles.

For a given polydisperse sedimentation model, expressed by the specific algebraic form of the flux vector $\mathbf{f}(\Phi)$, the ellipticity region (which usually has to be determined numerically [22]) for given particle densities and sizes should agree with those concentration regions for which instabilities have been observed experimentally. On the other hand, the model equations should be strictly hyperbolic for arbitrary N and equal-density particles. In [22] we show that the MLB model satisfies the first of these properties and is, in particular, not hyperbolic in general for suspensions in which two or more species have different densities. However, in [22] we were able to prove strict hyperbolicity for the system (1.4) with equal-density particles in the case $N = 2$ only. We indicated in [22] that numerical tests with $N = 3$ never produced an instability region, and we conjectured that the MLB equations were hyperbolic for arbitrary N, which is now proved in the present paper.

The properties of the MLB model contrast with those of several other models. For example, the model proposed by Davis and Gecol [38] again leads to a system of the form (1.4), but which for equal-density particles is hyperbolic only for small values of d_1/d_2 (for example, for $N = 2$ the restriction is $d_1/d_2 < 5$; see [22]), and for which the size of the ellipticity region drastically increases when d_1/d_2 is increased. Since no instabilities have been observed experimentally with equal-density suspensions, these ellipticity regions are unphysical and limit the use of the Davis and Gecol model to small values of d_1/d_2. We refer to [22] for a thorough discussion of mixed systems modeling polydisperse sedimentation and the consequences for the mathematical analysis.

In section 4, we consider the right-hand side of (1.2) using the diffusion matrix $\mathbf{A}(\Phi)$ derived in section 2. While it is obvious that $\mathbf{A}(\Phi) = 0$ on $\mathcal{D}_{\phi_c}$, it is not apparent that $\mathbf{A}(\Phi)$ is positive definite on $\mathcal{D}^0_{\phi_{\max}} \backslash \mathcal{D}_{\phi_c}$. The hyperbolicity and parabolicity properties of (1.2) associated with the matrices $\boldsymbol{\mathcal{J}}_{\mathbf{f}^M}(\Phi)$ and $\mathbf{A}(\Phi)$ are controlled by the independent model functions $V(\phi)$ and $\sigma_e(\phi)$, but their entries are analogous. Thus, the formula for the characteristic polynomial of $\boldsymbol{\mathcal{J}}_{\mathbf{f}^M}(\Phi)$ derived in section 3 also provides (after substitutions) a formula for that of $\mathbf{A}(\Phi)$. It is then straightforward to prove that $\mathbf{A}(\Phi)$ has N distinct nonnegative eigenvalues, which are positive if $\phi_c < \phi < \phi_{\max}$. Thus, (1.2) is strictly parabolic for $\phi_c < \phi < \phi_{\max}$, which is the main result of section 4.

In contrast to the hyperbolicity of the first-order system (1.4), the parabolicity property established in section 4 does not admit a direct physical interpretation. Rather, parabolicity is a condition ensuring the well-posedness (existence, uniqueness,

and stability) of systems of PDEs of the form (1.2). It should, however, be pointed out that mathematically rigorous well-posedness results are available for certain special cases of (1.2) only. These include, on one hand, *scalar* strongly degenerate parabolic-hyperbolic equations [6, 7, 8, 17, 25, 31, 61, 62, 72, 118], and, on the other hand, certain *uniformly parabolic* systems, that is, systems that do not degenerate into first-order type [42, 49, 63, 66]. A closed mathematical theory for the strongly degenerate systems considered in this paper is not available despite the increased interest this kind of equation has attained in recent years. Section 5 provides a short overview of the existing literature on mathematical and numerical theory for strongly degenerate parabolic problems.

In section 6, we first describe the central difference scheme due to Kurganov and Tadmor [64], which is used in this paper. The system (1.2) is discretized by a high-resolution central difference (Riemann solver free) scheme for the convection part (corresponding to the first-order equation (1.4)) combined with a central difference discretization of the parabolic parts (the right-hand side of (1.2)). Then we illustrate the (new) model of polydisperse sedimentation with compression by numerical examples with $N = 3$ and compare the results with simulations of the two (conventional) models of settling of monodisperse flocculated and polydisperse rigid-sphere suspensions (where $\sigma_{\mathrm{e}} \equiv 0$). We refer to [14, 19] for the application of similar numerical schemes to first-order systems like (1.4) describing sedimentation of polydisperse suspensions without compression effects.

The closing section 7 discusses various aspects of the paper. We first show that the type analysis of sections 3 and 4 is also valid in several space dimensions. Next, we briefly comment on the possible extension of the model to polydisperse suspensions with particles of different densities, and we furthermore provide a physical interpretation of one of the eigenvalue bounds derived in section 3. One frequent topic in the sedimentation literature is hydrodynamic diffusion, which is associated with particle velocity fluctuations. We give a brief survey of the literature on hydrodynamic diffusion and provide justification for not including this effect in our model. An important new property of the model is the prediction of diffusive relative movement of the different solids species within the sediment. This effect is clearly visible in the numerical simulations, which correspond to a hypothetical material, and may be less pronounced for real materials. We therefore discuss several alternative gradual and structural modifications of the present model that could reduce sediment diffusivity. Finally, some applications in which the sediment compressibility is important are discussed.

2. Derivation of the model of polydisperse sedimentation with compression.

2.1. Mass and linear momentum balance equations. A suspension may be represented as a superposition of continuous media, each following its own movement with the only restrictions imposed by the interaction between components. Each component obeys the laws of conservation of mass and momentum, incorporating terms to account for the interchange between components [27]. We assume that there is no mass transfer between species.

The local mass balance equations of the solid species and of the fluid can be written as

$$\frac{\partial \phi_i}{\partial t} + \nabla \cdot \big(\phi_i \mathbf{v}_i\big) = 0, \quad i = 1, \ldots, N, \qquad -\frac{\partial \phi}{\partial t} + \nabla \cdot \big((1-\phi)\mathbf{v}_{\mathrm{f}}\big) = 0, \tag{2.1}$$

where $\mathbf{v}_i$ is the phase velocity of solids species i, $i = 1, \dots, N$, and $\mathbf{v}_\mathrm{f}$ is the fluid phase velocity. Defining the volume-average velocity of the mixture $\mathbf{q} := (1-\phi)\mathbf{v}_\mathrm{f} + \phi_1\mathbf{v}_1 + \cdots + \phi_N\mathbf{v}_N$ and the relative velocities or slip velocities $\mathbf{u}_i := \mathbf{v}_i - \mathbf{v}_\mathrm{f}$ for $i = 1, \dots, N$, we derive easily that

$$\phi_i\mathbf{v}_i = \phi_i\big(\mathbf{u}_i + \mathbf{q} - (\phi_1\mathbf{u}_1 + \cdots + \phi_N\mathbf{u}_N)\big), \quad i = 1, \dots, N; \tag{2.2}$$

hence the solids mass balance equations can be rewritten in terms of $\mathbf{q}$ and $\mathbf{u}_1, \dots, \mathbf{u}_N$ as

$$\frac{\partial\phi_i}{\partial t} + \nabla\cdot\big(\phi_i\mathbf{u}_i + \phi_i\mathbf{q} - \phi_i(\phi_1\mathbf{u}_1 + \cdots + \phi_N\mathbf{u}_N)\big) = 0, \quad i = 1, \dots, N. \tag{2.3}$$

The sum of all equations in (2.1) produces the simple mass balance of the mixture, $\nabla\cdot\mathbf{q} = 0$. The momentum balance equations for the N solid species and the fluid are

$$\varrho_i\phi_i\frac{\mathrm{D}\mathbf{v}_i}{\mathrm{D}t} = \nabla\cdot\mathbf{T}_i + \varrho_i\phi_i\mathbf{b} + \mathbf{m}_i^\mathrm{f} + \mathbf{m}_i^\mathrm{s}, \quad i = 1, \dots, N, \tag{2.4}$$

$$\varrho_\mathrm{f}(1-\phi)\frac{\mathrm{D}\mathbf{v}_\mathrm{f}}{\mathrm{D}t} = \nabla\cdot\mathbf{T}_\mathrm{f} + \varrho_\mathrm{f}(1-\phi)\mathbf{b} - (\mathbf{m}_1^\mathrm{f} + \cdots + \mathbf{m}_N^\mathrm{f}). \tag{2.5}$$

Here ϱ_f is the mass density of the fluid, $\mathbf{T}_i$ denotes the stress tensor of particle species i, $i = 1, \dots, N$, $\mathbf{T}_\mathrm{f}$ that of the fluid, $\mathbf{b}$ is the body force, $\mathbf{m}_i^\mathrm{f}$ and $\mathbf{m}_{ij}^\mathrm{s}$ are the interaction forces per unit volume between solid species i and the fluid and between the solid species i and j, respectively, $\mathbf{m}_i^\mathrm{s} := \mathbf{m}_{i1}^\mathrm{s} + \cdots + \mathbf{m}_{iN}^\mathrm{s}$ is the particle-particle interaction term of species i, and we use the standard notation $\mathrm{D}\mathbf{v}/\mathrm{D}t := \partial\mathbf{v}/\partial t + (\mathbf{v}\cdot\nabla)\mathbf{v}$.

2.2. Solid and fluid stress tensors. We assume that the stress tensors of the solid and fluid phases can be written as $\mathbf{T}_i = -p_i\mathbf{I} + \mathbf{T}_i^\mathrm{E}$ for $i = 1, \dots, N$ and $\mathbf{T}_\mathrm{f} = -p_\mathrm{f}\mathbf{I} + \mathbf{T}_\mathrm{f}^\mathrm{E}$, respectively, where p_i denotes the phase pressure of particle species i, p_f that of the fluid, $\mathbf{I}$ denotes the identity tensor, and $\mathbf{T}_i^\mathrm{E}$ and $\mathbf{T}_\mathrm{f}^\mathrm{E}$ are the corresponding extra (or viscous) stress tensors, all of which could be given by expressions that correspond, for example, to a viscous-linear fluid. Since the focus here is on the continuity equations for the solids and we assume that viscous effects due to the motion of the mixture are not dominant, all viscous effects are assigned to the fluid extra-stress tensor. To make this simplification visible in the dimensional analysis, we assume that ν_0^f and $\nu_0^\mathrm{s} < \nu_0^\mathrm{f}$ are characteristic viscosities associated with the fluid and the solid species, respectively.

2.3. Partial pressures, pore pressure, and effective solid stress. The phase pressures $p_1, \dots, p_N$ and p_f are theoretical variables (arising from the averaging procedure [27]), which cannot be measured experimentally. As in [26], they are replaced by the pore pressure p and the effective solid stress σ_e, which are measurable. We assume that σ_e is given by a constitutive equation $\sigma_\mathrm{e} = \sigma_\mathrm{e}(\Phi)$, that is, as a function of the local composition of the sediment. To our knowledge (see also [102]), no suitable function $\sigma_\mathrm{e} = \sigma_\mathrm{e}(\Phi)$ for the polydisperse case has been derived either theoretically or empirically so far. However, most researchers utilize formulas that relate σ_e to the sediment porosity or, equivalently, to the total volumetric solids concentration ϕ [74, 98].

In stating the generic assumptions on σ_e, we follow [81, 92] and consider that during sedimentation, when $\phi \le \phi_\mathrm{c}$, there is no permanent contact between the particles (or aggregates of them), and the momentum transfer between the particles occurs entirely through the fluid or through collisions (although in a moment we shall

show that the latter effect is negligible here). This means that the total stress of the mixture, p_t, which can be decomposed in two different ways as

$$p_\mathrm{t} = p_\mathrm{f} + p_1 + \cdots + p_N = p + \sigma_\mathrm{e}(\phi), \tag{2.6}$$

equals the pore pressure, and therefore $\sigma_\mathrm{e}(\phi) = 0$ for $\phi \le \phi_\mathrm{c}$. (The second equality in (2.6) reflects the well-known effective-stress principle [39].) During consolidation, when $\phi > \phi_\mathrm{c}$, permanent contact is established between the solid particles, and the contact forces are transmitted through solid-solid contacts. Moreover, it can be assumed that the part of the total stress supported by the skeleton of networked solid particles is an increasing function of their concentration ϕ, i.e., $\sigma_\mathrm{e}'(\phi) := d\sigma_\mathrm{e}(\phi)/d\phi > 0$ for $\phi > \phi_\mathrm{c}$. These generic assumptions on $\sigma_\mathrm{e}(\phi)$ can be summarized as

$$\sigma_\mathrm{e}(\phi) \begin{cases} = 0 & \text{for } \phi \le \phi_\mathrm{c}, \\ > 0 & \text{for } \phi > \phi_\mathrm{c}, \end{cases} \qquad \sigma_\mathrm{e}'(\phi) \begin{cases} = 0 & \text{for } \phi \le \phi_\mathrm{c}, \\ > 0 & \text{for } \phi > \phi_\mathrm{c}; \end{cases} \tag{2.7}$$

a specific example is given in section 6. Our concept of effective solid stress has been adopted from soil consolidation theory [81, 92] but is consistent with and in some cases mathematically equivalent to the concepts of compressive yield stress [52, 67], effective pressure [40], or yield pressure [54] utilized by research workers with a focus on solid-liquid separation. All these papers have in common that it is assumed that the effective stress takes positive values if and only if the particles are networked, and that this occurs when $\phi > \phi_\mathrm{c}$, where ϕ_c is a distinct critical concentration, also called the "threshold value" or "gel point."

We now relate the fluid and solid phase pressures p_f and $p_1, \ldots, p_N$ to the effective solid stress σ_e and the pore pressure p. While p is defined within the fluid filling the interstices between the solids, the partial fluid pressure p_f is defined in the fluid component occupying the whole volume of the mixture. Let S be the cross-section of a settling column and $S_\mathrm{f} \subset S$ be its part that is filled out by the fluid in the porous medium, and let ϵ denote the surface porosity $\epsilon := |S_\mathrm{f}|/|S|$, i.e., $dS_\mathrm{f} = \epsilon dS$. Then the surface forces exerted on the fluid in a cross section of the sediment are

$$\int_S p_\mathrm{f}\, dS = \int_{S_\mathrm{f}} p\, dS_\mathrm{f} = \int_S p(\epsilon dS). \tag{2.8}$$

Since we may assume that the surface porosity equals the volume porosity [22], we may replace ϵ by $1 - \phi$, and as a consequence of the localization theorem [53], we obtain $p_\mathrm{f} = (1 - \phi)p$ from (2.8).

The effective solid stress σ_e is that part of the total stress p_t which acts on the porous network formed by the solid particles. Assuming that the cross-sectional surface area fraction of each solids species equals its volume fraction [22], we may conclude that $(\phi_i/\phi)\sigma_\mathrm{e}(\phi)$ is that part of σ_e which acts on species i. In view of $p_\mathrm{f} = (1 - \phi)p$, (2.6) may be rewritten as

$$p_1 + \cdots + p_N = \phi p + \frac{\phi_1 + \cdots + \phi_N}{\phi} \sigma_\mathrm{e}(\phi).$$

Thus, the phase pressure p_i is related to p and σ_e by $p_i = (\phi_i/\phi)(\phi p + \sigma_\mathrm{e}(\phi))$ for $i = 1, \ldots, N$.

2.4. Body force, solid-fluid, and particle-particle interaction forces. We assume that the only body force is gravity, $\mathbf{b} = -g\mathbf{k}$, where g is the acceleration of

gravity and $\mathbf{k}$ is the upwards-pointing unit vector. Furthermore, for a monodisperse suspension [26, 27, 34, 35], the interaction force $\mathbf{m}$ between the fluid and the unique solid phase can be modeled by

$$\mathbf{m} = \alpha(\phi)\mathbf{u} + \beta(\phi)\nabla\phi, \tag{2.9}$$

where α is the resistance coefficient and $\mathbf{u} := \mathbf{v}_\mathrm{s} - \mathbf{v}_\mathrm{f}$ is the solid-fluid relative or slip velocity. Equation (2.9) follows from the theorem of representation of isotropic functions [70, 99, 115, 115A, 115B] if we require that $\mathbf{m}$ be given as the most general linear function of $\mathbf{u}$, ϕ, and $\nabla\phi$. A similar result is obtained in [41], and (2.9) is also presented in [82] within a discussion of general principles for the formulation of constitutive equations. The function $\beta(\phi)$ can be shown to coincide with the pore pressure p (see [26]). In the present case, we analogously assume that the solid-fluid interaction term related to species i is given by $\mathbf{m}_i^\mathrm{f} = \alpha_i(\Phi)\mathbf{u}_i + \beta_i(\Phi)\nabla\phi_i$, where α_i is the resistance coefficient for the transfer of momentum between the fluid and solid phase species i, $i = 1, \dots, N$.

The interaction force between the different solid particle species could be specified by the Nakamura and Capes formula [1, 76, 98]:

$$\mathbf{m}_{ij}^\mathrm{s} = \frac{3}{2}\varphi_\mathrm{e}\frac{\varrho_i\varrho_j\phi_i\phi_j(d_i+d_j)^2}{\varrho_i d_i^3 + \varrho_j d_j^3}\,\|\mathbf{v}_i - \mathbf{v}_j\|\,(\mathbf{v}_i - \mathbf{v}_j), \quad i,j = 1,\dots,N, \quad i \neq j,$$

where the parameter φ_e accounts for non–head-on collisions [98] and its value depends on whether these are plastic or elastic. Typical values of φ_e vary between 0 and 5 [1, 76], and numerical simulations have not turned out to be sensitive to φ_e (see [1]). Nevertheless, the elimination of the term $\mathbf{m}_i^\mathrm{s} = \mathbf{m}_{i1}^\mathrm{s} + \cdots + \mathbf{m}_{iN}^\mathrm{s}$ due to the dimensional analysis (see section 2.5) is not dependent on any particular formula, since there is considerable experimental and theoretical evidence (summarized in [22]) that $\mathbf{m}_{ij}^\mathrm{s}$ can be neglected at the very low Reynolds numbers considered here.

To determine $\beta_1(\Phi), \dots, \beta_N(\Phi)$, we insert the constitutive assumptions into (2.4) and (2.5) and consider the mixture at equilibrium ($t \to \infty$) in a settling column. This state is characterized by $\mathbf{v}_\mathrm{f} = 0$, $\mathbf{u}_1 = \cdots = \mathbf{u}_N = 0$, and $\nabla p = -\varrho_\mathrm{f} g\mathbf{k}$, and we obtain $\beta_1(\Phi) = \cdots = \beta_N(\Phi) = p$; i.e., the functions β_i are all constant with respect to Φ [22, 26]. The linear momentum balances now read

$$\varrho_i\phi_i\frac{\mathrm{D}\mathbf{v}_i}{\mathrm{D}t} = -\varrho_i\phi_i g\mathbf{k} + \nabla\cdot\mathbf{T}_i^\mathrm{E} - \phi_i\nabla p + \alpha_i(\Phi)\mathbf{u}_i + \mathbf{m}_i^\mathrm{s} - \nabla\left(\frac{\phi_i}{\phi}\sigma_\mathrm{e}(\phi)\right), \quad i = 1,\dots,N, \tag{2.10}$$

$$\nabla p = -\varrho_\mathrm{f} g\mathbf{k} - \frac{1}{1-\phi}\big(\alpha_1(\Phi)\mathbf{u}_1 + \cdots + \alpha_N(\Phi)\mathbf{u}_N\big) - \varrho_\mathrm{f}\frac{\mathrm{D}\mathbf{v}_\mathrm{f}}{\mathrm{D}t} + \frac{1}{1-\phi}\nabla\cdot\mathbf{T}_\mathrm{f}^\mathrm{E}. \tag{2.11}$$

2.5. Dimensional analysis. We introduce dimensionless (starred) variables by referring all densities to ϱ_f, all velocities to the velocity U, all lengths to a typical length L, all solid and fluid viscosities to ν_0^s and ν_0^f, respectively, and all pressures to the hydrostatic pressure $\varrho_\mathrm{f} gL$. Here, we assume that U is the settling velocity of a single particle of the fastest settling species in an unbounded medium, and L is the depth of the settling vessel. A characteristic time is then given by $T = L/U$. A dimensionless gradient of a variable u is defined by $\nabla^* u = L\nabla u$, and a dimensionless time derivative by $\partial u/\partial t^* = T\partial u/\partial t = (L/U)\partial u/\partial t$. Using the Froude number of the flow $\mathrm{Fr} := U^2/(gL)$ and the sedimentation Reynolds number $\mathrm{Re} := dU/\nu_0^\mathrm{f}$, where d

is the size of the largest particles, we obtain from (2.4) and (2.11) the dimensionless equations

$$\begin{aligned}\varrho_i^*\phi_i\mathrm{Fr}\frac{\mathrm{D}\mathbf{v}_i^*}{\mathrm{D}t^*} =& -\varrho_i^*\phi_i\mathbf{k}+\frac{d}{L}\frac{\nu_0^{\mathrm{s}}}{\nu_0^{\mathrm{f}}}\frac{\mathrm{Fr}}{\mathrm{Re}}\nabla^*\cdot\left(\mathbf{T}_i^{\mathrm{E}}\right)^*-\phi_i\nabla^*p^*+\alpha_i^*(\Phi)\mathbf{u}_i^*\\ &+\frac{L}{d}\mathrm{Fr}(\mathbf{m}_i^{\mathrm{s}})^*-\nabla^*\left(\frac{\phi_i}{\phi}\sigma_{\mathrm{e}}^*(\phi)\right),\quad i=1,\ldots,N,\end{aligned}\tag{2.12}$$

$$\nabla^*p^*=-\mathbf{k}-\frac{1}{1-\phi}\left(\alpha_1^*(\Phi)\mathbf{u}_1^*+\cdots+\alpha_N^*(\Phi)\mathbf{u}_N^*\right)-\mathrm{Fr}\frac{\mathrm{D}\mathbf{v}_{\mathrm{f}}^*}{\mathrm{D}t^*}+\frac{1}{1-\phi}\frac{d}{L}\frac{\mathrm{Fr}}{\mathrm{Re}}\nabla^*\cdot\left(\mathbf{T}_{\mathrm{f}}^{\mathrm{E}}\right)^*.\tag{2.13}$$

The values $d=10^{-4}\,\mathrm{m}$, $g=10\,\mathrm{m/s^2}$, $L=1\,\mathrm{m}$ (height of a settling vessel), $U=10^{-4}\,\mathrm{m/s}$ (settling velocity of a particle of the fastest species in an unbounded fluid), and $\nu_0^{\mathrm{f}}=10^{-6}\,\mathrm{m^2/s}$ (kinematic viscosity of water) are typical for the particulate systems considered here and imply $\mathrm{Fr}=10^{-9}$, $\mathrm{Re}=10^{-2}$, and $d/L=10^{-4}$. Since all viscous effects have been moved onto the fluid extra-stress tensor, we can assume $\nu_0^{\mathrm{s}}/\nu_0^{\mathrm{f}}\ll 1$. We assume that all dimensionless variables are of the order of magnitude $\mathcal{O}(1)$. Then we obtain, by discarding from (2.12) all terms that have a coefficient that is 10^{-5} or smaller, and discarding the advective acceleration term from (2.13) but retaining the viscous term, the following simplified linear momentum balances:

$$\alpha_i(\Phi)\mathbf{u}_i=\varrho_i\phi_i g\mathbf{k}+\phi_i\nabla p+\nabla\left(\frac{\phi_i}{\phi}\sigma_{\mathrm{e}}(\phi)\right),\quad i=1,\ldots,N,\tag{2.14}$$

$$\nabla p=-\varrho_{\mathrm{f}}g\mathbf{k}-\frac{1}{1-\phi}\left(\alpha_1(\Phi)\mathbf{u}_1+\cdots+\alpha_N(\Phi)\mathbf{u}_N\right)+\frac{1}{1-\phi}\nabla\cdot\mathbf{T}_{\mathrm{f}}^{\mathrm{E}},\tag{2.15}$$

which are written again in their dimensional forms. The small viscous term $\nabla\cdot\mathbf{T}_{\mathrm{f}}^{\mathrm{E}}$ is retained in (2.15) when this equation acts as an equation for the motion of the mixture. We shall comment on the necessity of viscous terms in the multidimensional case in section 2.7.

The term $\nabla\cdot\mathbf{T}_{\mathrm{f}}^{\mathrm{E}}$ is, however, deleted when (2.15) is inserted into (2.14), in order to produce a solvable linear system for the slip velocities $\mathbf{u}_1,\ldots,\mathbf{u}_N$. Thus, this system can be written as

$$\begin{aligned}&\frac{\alpha_i(\Phi)(1-\phi)}{\phi_i}\mathbf{u}_i+\sum_{j=1}^{N}\alpha_j(\Phi)\mathbf{u}_j\\ &=(1-\phi)\left[\left(\varrho_i-\varrho_{\mathrm{f}}\right)g\mathbf{k}+\frac{1}{\phi_i}\nabla\left(\frac{\phi_i}{\phi}\sigma_{\mathrm{e}}(\phi)\right)\right],\quad i=1,\ldots,N.\end{aligned}\tag{2.16}$$

2.6. Explicit formula for the slip velocities $\mathbf{u}_i$. Let $\varrho(\Phi):=(1-\phi)\varrho_{\mathrm{f}}+\phi_1\varrho_1+\cdots+\phi_N\varrho_N$ denote the local density of the mixture, and note that $\phi_1(\varrho_1-\varrho_{\mathrm{f}})+\cdots+\phi_N(\varrho_N-\varrho_{\mathrm{f}})=\varrho(\Phi)-\varrho_{\mathrm{f}}$. Then the following explicit equation for the slip velocities $\mathbf{u}_i$ as functions of Φ is obtained as the solution of the system (2.16), which follows from the Sherman–Morrison formula [22]:

$$\mathbf{u}_i=\frac{\phi_i}{\alpha_i(\Phi)}\left[\left(\varrho_i-\varrho(\Phi)\right)g\mathbf{k}+\frac{\sigma_{\mathrm{e}}(\phi)}{\phi_i}\nabla\left(\frac{\phi_i}{\phi}\right)+\frac{1-\phi}{\phi}\nabla\sigma_{\mathrm{e}}(\phi)\right],\quad i=1,\ldots,N.\tag{2.17}$$

Following [22] and being consistent with Masliyah [73] and Lockett and Bassoon [71], we choose $\phi_i/\alpha_i(\Phi)=-d_i^2V(\Phi)/(18\mu_{\mathrm{f}})$, where μ_{f} is the viscosity of the pure fluid, and

the hindered settling factor $V(\Phi)$ can, for example, be chosen as $V(\Phi) = (1-\phi)^{n(\Phi)-2}$ [86]. Since the dependence of n on Φ is through wall effects, which are small when d is very small compared to the diameter of the settling vessel, we may limit the analysis to formulas of the type $V(\Phi) = V(\phi)$ and obtain

$$\mathbf{u}_i = -\frac{d_i^2}{18\mu_{\mathrm{f}}} V(\phi)\left[\big(\varrho_i - \varrho(\Phi)\big) g\mathbf{k} + \frac{\sigma_{\mathrm{e}}(\phi)}{\phi_i}\nabla\Big(\frac{\phi_i}{\phi}\Big) + \frac{1-\phi}{\phi}\nabla\sigma_{\mathrm{e}}(\phi)\right], \quad i = 1, \dots, N. \tag{2.18}$$

The generic assumption to ensure hyperbolicity, which is satisfied by $V(\phi) = (1-\phi)^{n-2}$, $n > 2$, is

$$V(\phi) > 0, \quad V'(\phi) < 0 \quad \text{for } 0 < \phi < \phi_{\max}. \tag{2.19}$$

2.7. Final form of the model equations. The final model equations are the continuity equations of the solids species and of the mixture ($\nabla \cdot \mathbf{q} = 0$), the linear momentum balance of the fluid (2.15), and the equations (2.18) for the slip velocities $\mathbf{u}_i$ derived from the linear momentum balances of the solid species. To derive explicit expressions for the fluxes $\phi_1\mathbf{v}_1, \dots, \phi_N\mathbf{v}_N$ appearing in these equations, we introduce the reduced densities $\bar{\varrho}_{\mathrm{s}} := \varrho_{\mathrm{s}} - \varrho_{\mathrm{f}}$, where ϱ_{s} is the density of the solid particles if they differ only in size, $\bar{\varrho}_i := \varrho_i - \varrho_{\mathrm{f}}$, $i = 1, \dots, N$, the vector $\bar{\boldsymbol{\varrho}} := (\bar{\varrho}_1, \dots, \bar{\varrho}_N)^{\mathrm{T}}$, and the parameters $\mu := -gd_1^2/(18\mu_{\mathrm{f}})$ and $\delta_i := d_i^2/d_1^2$, $i = 1, \dots, N$, such that (2.18) reads

$$\mathbf{u}_i = \mu\delta_i V(\phi)\left[(\bar{\varrho}_i - \bar{\boldsymbol{\varrho}}^{\mathrm{T}}\Phi)\mathbf{k} + \frac{\sigma_{\mathrm{e}}(\phi)}{g\phi_i}\nabla\Big(\frac{\phi_i}{\phi}\Big) + \frac{1-\phi}{g\phi}\nabla\sigma_{\mathrm{e}}(\phi)\right], \quad i = 1, \dots, N. \tag{2.20}$$

From (2.2), we get $\phi_i\mathbf{v}_i = f_i^{\mathrm{M}}(\Phi)\mathbf{k} + \phi_i\mathbf{q} - \mathbf{a}_i(\Phi, \nabla\Phi)$ for $i = 1, \dots, N$, where the components of $\mathbf{f}^{\mathrm{M}}(\Phi)$ (corresponding to the MLB model for suspensions of rigid spheres) are given by

$$f_i(\Phi) = f_i^{\mathrm{M}}(\Phi) = \mu V(\phi)\phi_i\left[\delta_i(\bar{\varrho}_i - \bar{\boldsymbol{\varrho}}^{\mathrm{T}}\Phi) - \sum_{k=1}^{N}\delta_k\phi_k(\bar{\varrho}_k - \bar{\boldsymbol{\varrho}}^{\mathrm{T}}\Phi)\right], \quad i = 1, \dots, N. \tag{2.21}$$

If we let $\boldsymbol{\delta} := (\delta_1, \dots, \delta_N)^{\mathrm{T}}$, then the vectors $\mathbf{a}_i(\Phi, \nabla\Phi)$ are given by

$$\begin{aligned}\mathbf{a}_i(\Phi, \nabla\Phi) = -\frac{\mu V(\phi)}{g}\Bigg\{&\frac{(1-\phi)\phi_i}{\phi}(\delta_i - \boldsymbol{\delta}^{\mathrm{T}}\Phi)\nabla\sigma_{\mathrm{e}}(\phi) \\ &+ \sigma_{\mathrm{e}}(\phi)\left[\delta_i\nabla\Big(\frac{\phi_i}{\phi}\Big) - \phi_i\left(\delta_1\nabla\Big(\frac{\phi_1}{\phi}\Big) + \cdots + \delta_N\nabla\Big(\frac{\phi_N}{\phi}\Big)\right)\right]\Bigg\}, \quad i = 1, \dots, N.\end{aligned} \tag{2.22}$$

The continuity equations for the solids, i.e., for the N unknowns ϕ_1 to ϕ_N, can then be written as

$$\frac{\partial\phi_i}{\partial t} + \nabla\cdot\big(\phi_i\mathbf{q} + f_i^{\mathrm{M}}(\Phi)\mathbf{k}\big) = \nabla\cdot\mathbf{a}_i(\Phi, \nabla\Phi), \quad i = 1, \dots, N. \tag{2.23}$$

Due to the property (2.7), $\mathbf{a}_i(\Phi, \nabla\Phi) = 0$ wherever $\phi \le \phi_{\mathrm{c}}$. At these concentrations, the system (2.23) turns into the first-order system of N scalar equations analyzed in

[22]. The final coupled set of model equations, valid in several space dimensions, is given by (2.23) and the equations

$$\nabla \cdot \mathbf{q} = 0, \tag{2.24}$$

$$\begin{aligned} \nabla p =& -\nabla \sigma_{\mathrm{e}}(\phi) - (\varrho_{\mathrm{f}} + \bar{\boldsymbol{\varrho}} \cdot \Phi) g \mathbf{k} + \frac{1}{1-\phi} \nabla \cdot \mathbf{T}_{\mathrm{f}}^{\mathrm{E}} \\ \equiv& -\nabla \sigma_{\mathrm{e}}(\phi) - \varrho(\Phi) g \mathbf{k} + \frac{1}{1-\phi} \nabla \cdot \mathbf{T}_{\mathrm{f}}^{\mathrm{E}}. \end{aligned} \tag{2.25}$$

Before discussing the role of (2.25), we set $N = 1$ to check consistency with the model of sedimentation of monodisperse flocculated suspensions [26]. With

$$f^{\mathrm{M}}(\phi) = -\frac{g d^2 \bar{\varrho}_{\mathrm{s}}}{18 \mu_{\mathrm{f}}} V(\phi) \phi (1-\phi)^2, \quad \mathbf{a}(\phi, \nabla\phi) = a(\phi) \nabla \phi = -\frac{f^{\mathrm{M}}(\phi)}{\bar{\varrho}_{\mathrm{s}} g \phi} \nabla \sigma_{\mathrm{e}}(\phi),$$

$$a(\phi) = -\frac{f^{\mathrm{M}}(\phi) \sigma_{\mathrm{e}}'(\phi)}{\bar{\varrho}_{\mathrm{s}} g \phi},$$

we see that (2.23) indeed reduces to the scalar equation

$$\frac{\partial \phi}{\partial t} + \nabla \cdot \big(\phi \mathbf{q} + f^{\mathrm{M}}(\phi) \mathbf{k} \big) = \nabla \cdot \big(a(\phi) \nabla \phi \big) \tag{2.26}$$

derived in [26]. It is easy to see that (2.26) is first-order hyperbolic for $\phi \le \phi_{\mathrm{c}}$ and $\phi = 1$, and second-order parabolic for $\phi_{\mathrm{c}} < \phi < 1$, and therefore a strongly degenerate parabolic equation.

Noting that $\mathbf{v}_{\mathrm{f}} = \mathbf{q} - (\phi_1 \mathbf{u}_1 + \cdots + \phi_N \mathbf{u}_N)$, we can rewrite $\mathbf{T}_{\mathrm{f}}^{\mathrm{E}}$ in terms of the mixture velocity $\mathbf{q}$ and the slip velocities $\mathbf{u}_i$, which are now given functions of Φ. For example, if we use the expression $\mathbf{T}_{\mathrm{f}}^{\mathrm{E}} = \mu(\phi)[\nabla \mathbf{v}_{\mathrm{f}} + (\nabla \mathbf{v}_{\mathrm{f}})^{\mathrm{T}} - (2/3)(\nabla \cdot \mathbf{v}_{\mathrm{f}})\mathbf{I}]$ as for a standard viscous-linear fluid but with a concentration-dependent viscosity function, then (2.25) can be rewritten in the form

$$\nabla p = -\varrho(\Phi) g \mathbf{k} + \frac{1}{1-\phi} \Big[\big(\nabla \mu(\phi) \big)^{\mathrm{T}} \big(\nabla \mathbf{q} + (\nabla \mathbf{q})^{\mathrm{T}} \big) + \mu(\phi) \Delta \mathbf{q} \Big] + \mathbf{g}(\Phi, \nabla\Phi, \nabla^2\Phi), \tag{2.27}$$

where $\mathbf{g}$ is a function depending on Φ and the derivatives of its components of up to second order. For pure fluid, i.e., when $\Phi \equiv 0$ (and thus $\mathbf{q} \equiv \mathbf{v}_{\mathrm{f}}$), (2.24) and (2.25) form the Stokes system for an incompressible fluid for the velocity $\mathbf{q}$ and the pressure p.

We now comment on the necessity of retaining a viscosity term, such as $\mu(\phi)\Delta\mathbf{q}$ in (2.25) or (2.27). In fact, deleting *all* terms which are expected to be small according to the dimensional analysis would require that we consider the following equation instead of (2.25):

$$\nabla p = -\nabla \sigma_{\mathrm{e}}(\phi) - \varrho(\Phi) g \mathbf{k}. \tag{2.28}$$

To elucidate the consequences of (2.28), we take the curl of (2.28), which leads to $\partial \varrho(\Phi)/\partial x = \partial \varrho(\Phi)/\partial y = 0$, such that the local density of the mixture depends on height only [93]. For $N = 1$, the implications of this observation are well known [23, 93]. Although the concentration waves (kinematic waves) are one-dimensional, they are embedded in the three-dimensional mixture flow field $\mathbf{q}$. Since $\mathbf{q}$ does not appear in the field equation (2.28), the coupling between the flow field and the kinematic waves

has to be modeled by boundary conditions, which requires introducing boundary layers of sediment or streaming liquid. The resulting kinematic-wave theory has been useful in explaining the behavior of relatively dilute suspensions in vessels with inclined walls [93] or in centrifuges [90, 91]. In [23], this approach is extended to monodisperse suspensions with compressible sediments, for which numerical solutions can be readily obtained. However, it is also shown in [23] that the kinematic-wave theory does not lead to a mathematically well-posed problem, and that this shortcoming is due to the absence of the aforementioned coupling between kinematic waves and the flow field in (2.28). On the other hand, in [24], energy estimates for slight variants of the coupled system (2.23)–(2.25) with $N = 1$ are obtained. These estimates lead to existence and stability results, and follow from the viscosity term in (2.25).

We now consider one space dimension, for which we get $\partial q/\partial z = 0$, and only (2.23) needs to be solved, since q is given by boundary conditions and (2.25) turns into an equation for the pore pressure p, which permits us to calculate this quantity a posteriori from $\phi_1, \dots, \phi_N$.

2.8. Initial and boundary conditions in one space dimension. In a closed one-dimensional vessel, the mixture velocity at the bottom vanishes; hence $q \equiv 0$, and the remaining equations that actually have to be solved are the system of convection-diffusion equations

$$\frac{\partial \phi_i}{\partial t} + \frac{\partial f_i^{\mathrm{M}}(\Phi)}{\partial z} = \frac{\partial}{\partial z}\left[a_i\left(\Phi, \frac{\partial \Phi}{\partial z}\right)\right], \quad i = 1, \dots, N, \tag{2.29}$$

together with an initial concentration distribution and zero flux boundary conditions, i.e.,

$$\Phi(z, 0) = \Phi^0(z) \in \mathcal{D}_{\phi_{\max}}, \ \ 0 \le z \le L, \tag{2.30}$$

$$\phi_i v_i = f_i^{\mathrm{M}}(\Phi) - a_i\left(\Phi, \frac{\partial \Phi}{\partial z}\right) = 0 \quad \text{for } z = 0 \text{ and } z = L,\ i = 1, \dots, N. \tag{2.31}$$

3. Hyperbolicity of the first-order system. We now assume $\varrho_1 = \cdots = \varrho_N = \varrho_{\mathrm{s}}$, so that the components of $\mathbf{f}^{\mathrm{M}}(\Phi)$ are

$$f_i^{\mathrm{M}}(\Phi) = \mu \bar{\varrho}_{\mathrm{s}} V(\phi)(1 - \phi)(\delta_i - \boldsymbol{\delta}^{\mathrm{T}}\Phi)\phi_i, \quad i = 1, \dots, N, \tag{3.1}$$

and we denote by $P(\lambda)$ the characteristic polynomial of $\mathbf{J} := (\mu\bar{\varrho}_{\mathrm{s}})^{-1}\boldsymbol{\mathcal{J}}_{\mathbf{f}^{\mathrm{M}}}(\Phi)$, where $\boldsymbol{\mathcal{J}}_{\mathbf{f}^{\mathrm{M}}}(\Phi) = (\partial f_i^{\mathrm{M}}(\Phi)/\partial\phi_j)_{i,j=1,\dots,N}$ is the Jacobian of $\mathbf{f}^{\mathrm{M}}(\Phi)$. We now derive a closed algebraic expression for $P(\lambda)$. We can write $(\mu\bar{\varrho}_{\mathrm{s}})^{-1}\partial f_i^{\mathrm{M}}(\Phi)/\partial\phi_j = \gamma_j^i(\Phi)\phi_i + \gamma^i(\Phi)\delta_{ij}$ for $i, j = 1, \dots, N$, where

$$\gamma^i(\Phi) := V(\phi)(1 - \phi)(\delta_i - \boldsymbol{\delta}^{\mathrm{T}}\Phi), \quad i = 1, \dots, N, \tag{3.2}$$

$$\gamma_j^i(\Phi) := \big(V(\phi)(1 - \phi)\big)'(\delta_i - \boldsymbol{\delta}^{\mathrm{T}}\Phi) - V(\phi)(1 - \phi)\delta_j, \quad i, j = 1, \dots, N. \tag{3.3}$$

The characteristic polynomial can be written as

$$P(\lambda) := \det(\mathbf{J} - \lambda\mathbf{I}) = \begin{vmatrix} \gamma_1^1\phi_1 + \gamma^1 - \lambda & \gamma_2^1\phi_1 & \cdots & \gamma_N^1\phi_1 \\ \gamma_1^2\phi_2 & \gamma_2^2\phi_2 + \gamma^2 - \lambda & \cdots & \gamma_N^2\phi_2 \\ \vdots & \vdots & \ddots & \vdots \\ \gamma_1^N\phi_N & \gamma_2^N\phi_N & \cdots & \gamma_N^N\phi_N + \gamma^N - \lambda \end{vmatrix}. \tag{3.4}$$

In what follows, we omit the argument Φ and, for later use, note that $\gamma^i - \gamma^l = V(\phi)(1-\phi)(\delta_i - \delta_l)$, which due to $\delta_1 > \delta_2 > \cdots > \delta_N$ implies $\gamma^N < \gamma^{N-1} < \cdots < \gamma^1$. Moreover, we observe that

$$\gamma_j^1 - \gamma_k^1 = \cdots = \gamma_j^N - \gamma_k^N = -V(\phi)(1-\phi)(\delta_j - \delta_k), \quad j,k = 1,\ldots,N,$$
$$\gamma_1^j - \gamma_1^k = \cdots = \gamma_N^j - \gamma_N^k = \big(V(\phi)(1-\phi)\big)'(\delta_j - \delta_k), \quad j,k = 1,\ldots,N.$$

The common values of $\gamma_j^i - \gamma_k^i$ and $\gamma_i^j - \gamma_i^k$ for all $i = 1,\ldots,N$, $j,k = 1,\ldots,N$, will be denoted by $\gamma_{j,k}$ and $\gamma^{j,k}$, respectively. Since $\boldsymbol{\mathcal{J}}_{\mathbf{f}^{\mathrm{M}}}(\Phi)$ and $\mathbf{A}(\Phi)$ have similar structure and therefore similar characteristic polynomials, it is convenient for later use to prove the following lemma separately.

LEMMA 3.1. *The polynomial $P(\lambda)$ defined in* (3.4) *satisfies*

$$P(\lambda) = \left\{1 + \sum_{m=1}^{N} \frac{\phi_m \gamma_m^m}{\gamma^m - \lambda} - \sum_{m=1}^{N} \frac{\phi_m}{\gamma^m - \lambda} \sum_{l=1}^{N} \frac{\phi_l \gamma_{l,N} \gamma^{l,m}}{\gamma^l - \lambda}\right\} \prod_{k=1}^{N} (\gamma^k - \lambda). \tag{3.5}$$

Proof. In this proof we merely use the definitions of $\gamma_{j,k}$ and $\gamma^{j,k}$ in terms of the γ_j^i's and γ_j's. Subtracting column N from columns 1 to $N-1$ in (3.4) yields

$$P(\lambda) = \begin{vmatrix} \gamma_{1,N}\phi_1 + \gamma^1 - \lambda & \cdots & \gamma_{N-1,N}\phi_1 & \gamma_N^1 \phi_1 \\ \vdots & \ddots & \vdots & \vdots \\ \gamma_{1,N}\phi_{N-1} & \cdots & \gamma_{N-1,N}\phi_{N-1} + \gamma^{N-1} - \lambda & \gamma_N^{N-1}\phi_{N-1} \\ \gamma_{1,N}\phi_N - \gamma^N + \lambda & \cdots & \gamma_{N-1,N}\phi_N - \gamma^N + \lambda & \gamma_N^N \phi_N + \gamma^N - \lambda \end{vmatrix}. \tag{3.6}$$

Expanding this determinant on the last row, we get

$$P(\lambda) = X + (\gamma^N - \lambda)(-1)^N \big(Y_1 - Y_2 + Y_3 - \cdots + (-1)^N Y_{N-1}\big), \tag{3.7}$$

where X and Y_m are the determinants obtained from the determinant in (3.6) by replacing the last row by $(\gamma_{1,N}\phi_N, \ldots, \gamma_{N-1,N}\phi_N, \gamma_N^N\phi_N + \gamma^N - \lambda)$ and by deleting the last row and the mth column, $m = 1,\ldots,N-1$, respectively. Multiplying the last row in X with $(-\phi_i/\phi_N)$ and adding the result to the ith row, $i = 1,\ldots,N-1$, leads to

$$X = \begin{vmatrix} \gamma^1 - \lambda & \cdots & 0 & \phi_1\big(\gamma^{1,N} - (\gamma^N - \lambda)/\phi_N\big) \\ \vdots & \ddots & \vdots & \vdots \\ 0 & \cdots & \gamma^{N-1} - \lambda & \phi_{N-1}\big(\gamma^{N-1,N} - (\gamma^N - \lambda)/\phi_N\big) \\ \gamma_{1,N}\phi_N & \cdots & \gamma_{N-1,N}\phi_N & \gamma_N^N\phi_N + \gamma^N - \lambda \end{vmatrix}.$$

Expanding X on the last row yields

$$X = \left(\gamma_N^N\phi_N + \gamma^N - \lambda - \phi_N \sum_{m=1}^{N-1} \frac{\phi_m \gamma_{m,N}}{\gamma^m - \lambda}\left(\gamma^{m,N} - \frac{\gamma^N - \lambda}{\phi_N}\right)\right) \prod_{k=1}^{N-1} (\gamma^k - \lambda). \tag{3.8}$$

Furthermore, we have $Y_m = (-1)^{N-1-m}\tilde{Y}_m$, where

$$\tilde{Y}_m = \begin{vmatrix} \gamma_{1,N}\phi_1 + \gamma^1 - \lambda & \cdots & \gamma_{m-1,N}\phi_1 & \gamma_{m+1,N}\phi_1 & \cdots & \gamma_{N-1,N}\phi_1 & \gamma_N^1\phi_1 \\ \vdots & \ddots & \vdots & \vdots & & \vdots & \vdots \\ \gamma_{1,N}\phi_{m-1} & \cdots & \gamma_{m-1,N}\phi_{m-1} + \gamma^{m-1} - \lambda & \gamma_{m+1,N}\phi_{m-1} & \cdots & \gamma_{N-1,N}\phi_{m-1} & \gamma_N^{m-1}\phi_{m-1} \\ \gamma_{1,N}\phi_{m+1} & \cdots & \gamma_{m-1,N}\phi_{m+1} & \gamma_{m+1,N}\phi_{m+1} + \gamma^{m+1} - \lambda & \cdots & \gamma_{N-1,N}\phi_{m+1} & \gamma_N^{m+1}\phi_{m+1} \\ \vdots & & \vdots & \vdots & \ddots & \vdots & \vdots \\ \gamma_{1,N}\phi_{N-1} & \cdots & \gamma_{m-1,N}\phi_{N-1} & \gamma_{m+1,N}\phi_{N-1} & \cdots & \gamma_{N-1,N}\phi_{N-1} + \gamma^{N-1} - \lambda & \gamma_N^{N-1}\phi_{N-1} \\ \gamma_{1,N}\phi_m & \cdots & \gamma_{m-1,N}\phi_m & \gamma_{m+1,N}\phi_m & \cdots & \gamma_{N-1,N}\phi_m & \gamma_N^m\phi_m \end{vmatrix},$$

which implies

$$Y_m = (-1)^{N-1-m}\frac{\phi_m}{\gamma^m - \lambda}\left(\gamma_N^m - \sum_{l=1}^{N-1}\frac{\gamma_{l,N}\gamma^{l,m}\phi_l}{\gamma^l - \lambda}\right)\prod_{k=1}^{N-1}(\gamma^k - \lambda),$$

$$m = 1, \dots, N-1. \tag{3.9}$$

Inserting (3.8) and (3.9) into (3.7), we get

$$\begin{aligned} P(\lambda) =& \left\{\gamma_N^N\phi_N + \gamma^N - \lambda - \phi_N\sum_{m=1}^{N-1}\frac{\phi_m}{\gamma^m - \lambda}\gamma_{m,N}\left(\gamma^{m,N} - \frac{\gamma^N - \lambda}{\phi_N}\right)\right. \\ &\left. + (\gamma^N - \lambda)\sum_{m=1}^{N-1}\frac{\phi_m}{\gamma^m - \lambda}\left(\gamma_N^m - \sum_{l=1}^{N-1}\phi_l\frac{\gamma_{l,N}\gamma^{l,m}}{\gamma^l - \lambda}\right)\right\}\prod_{k=1}^{N-1}(\gamma^k - \lambda) \\ =& \left\{1 - \frac{\phi_N}{\gamma^N - \lambda}\sum_{m=1}^{N-1}\frac{\phi_m\gamma_{m,N}\gamma^{m,N}}{\gamma^m - \lambda} + \sum_{m=1}^{N-1}\frac{\phi_m\gamma_{m,N}}{\gamma^m - \lambda}\right. \\ &\left. + \sum_{m=1}^{N}\frac{\phi_m\gamma_N^m}{\gamma^m - \lambda} - \sum_{m=1}^{N-1}\frac{\phi_m}{\gamma^m - \lambda}\sum_{l=1}^{N-1}\frac{\phi_l\gamma_{l,N}\gamma^{l,m}}{\gamma^l - \lambda}\right\}\prod_{l=1}^{N}(\gamma^l - \lambda). \end{aligned} \tag{3.10}$$

The upper index of summation in the second sum in the second equation of (3.10) can be changed to N since $\gamma_{N,N} = 0$, and the second and third sum can be combined into one using $\gamma_{m,N} + \gamma_N^m = \gamma_m^m$. Furthermore, the first and the fourth sums can be combined into one by changing the upper index of summation for m in the fourth sum from $N-1$ to N, from which we obtain (3.5). ∎

We can now prove the following lemma.

LEMMA 3.2. *Let $\lambda \in \mathbb{R}$ and $\delta(\lambda) := (V(\phi)(1-\phi))^{-1}\lambda + \boldsymbol{\delta}^{\mathrm{T}}\Phi$. Then $P(\lambda)$ is given by*

$$\begin{aligned} P(\lambda) =& \left\{V(\phi)(1-\phi) + \sum_{m=1}^{N}\frac{\phi_m}{\delta_m - \delta(\lambda)}\left[-\delta_m V(\phi)(1-\phi) + \big(V(\phi)(1-\phi)\big)'\right.\right. \\ &\left.\left. \times\left(\delta_m - \boldsymbol{\delta}^{\mathrm{T}}\Phi + \sum_{l=1}^{N}\frac{\delta_l\phi_l(\delta_l - \delta_m)}{\delta_l - \delta(\lambda)}\right)\right]\right\}\big(V(\phi)(1-\phi)\big)^{N-1}\prod_{k=1}^{N}\big(\delta_k - \delta(\lambda)\big). \end{aligned} \tag{3.11}$$

This expression is also well defined for $\lambda \in \{\gamma^1, \dots, \gamma^N\}$ and reads for $k = 1, \dots, N$ as

$$P(\gamma^k) = \phi_k\delta_k\Big\{\big(V(\phi)(1-\phi)\big)' - V(\phi)\Big\}\big(V(\phi)\big)^{N-1}(1-\phi)^N\prod_{\substack{l=1 \\ l\neq k}}^{N}(\delta_l - \delta_k). \tag{3.12}$$

Proof. Using $\gamma^m - \lambda = (\delta_m - \delta(\lambda))V(\phi)(1-\phi)$ and the definitions of $\gamma_{l,N}$ and $\gamma^{l,m}$, we get

(3.13)

$$\begin{aligned}
P(\lambda) =& \Bigg\{ 1 + \sum_{m=1}^{N} \frac{\phi_m[(V(\phi)(1-\phi))'(\delta_m - \boldsymbol{\delta}^{\mathrm{T}}\Phi) - V(\phi)(1-\phi)\delta_m]}{V(\phi)(1-\phi)(\delta_m - \delta(\lambda))} + \frac{(V(\phi)(1-\phi))'}{V(\phi)(1-\phi)} \\
&\times \sum_{m=1}^{N}\sum_{l=1}^{N} \frac{\phi_m\phi_l(\delta_l^2 - \delta_l\delta_m - \delta_l\delta_N + \delta_m\delta_N)}{(\delta_m - \delta(\lambda))(\delta_l - \delta(\lambda))} \Bigg\} \big(V(\phi)(1-\phi)\big)^N \prod_{k=1}^{N} \big(\delta_k - \delta(\lambda)\big) \\
=& \Bigg\{ V(\phi)(1-\phi) + \sum_{m=1}^{N} \frac{\phi_m}{\delta_m - \delta(\lambda)} \Bigg[-V(\phi)(1-\phi)\delta_m + \big(V(\phi)(1-\phi)\big)' \\
&\times \left(\delta_m - \boldsymbol{\delta}^{\mathrm{T}}\Phi + \sum_{l=1}^{N} \frac{\delta_l\phi_l(\delta_l - \delta_m)}{\delta_l - \delta(\lambda)} \right) \Bigg] \Bigg\} \big(V(\phi)(1-\phi)\big)^{N-1} \prod_{k=1}^{N} \big(\delta_k - \delta(\lambda)\big),
\end{aligned}$$

which is (3.11). This expression can be rewritten as

$$\begin{aligned}
P(\lambda) =& \prod_{l=1}^{N} (\gamma^l - \lambda) \\
&+ \Bigg\{ \sum_{m=1}^{N} \phi_m \Big[-\delta_m V(\phi)(1-\phi) + \big(V(\phi)(1-\phi)\big)'(\delta_m - \boldsymbol{\delta}^{\mathrm{T}}\Phi) \Big] \prod_{\substack{l=1 \\ l\neq m}}^{N} \big(\delta_l - \delta(\lambda)\big) \\
&+ \big(V(\phi)(1-\phi)\big)' \sum_{m=1}^{N}\sum_{l=1}^{N} \phi_m\phi_l\delta_l(\delta_l - \delta_m) \prod_{\substack{n=1 \\ n\neq m,l}}^{N} \big(\delta_n - \delta(\lambda)\big) \Bigg\} V(\phi)(1-\phi)^{N-1}.
\end{aligned}$$

For $\lambda = \gamma^k$ the first product vanishes, and in the first sum only the summand with $m = k$ and in the second sum only the summands with $m = k$ or $l = k$ do not vanish. This implies

$$\begin{aligned}
P(\gamma^k) =& \Bigg\{ \phi_k \Big[-\delta_k V(\phi)(1-\phi) + \big(V(\phi)(1-\phi)\big)'(\delta_k - \boldsymbol{\delta}^{\mathrm{T}}\Phi) \Big] \prod_{\substack{l=1 \\ l\neq k}}^{N} (\delta_l - \delta_k) \\
&+ \big(V(\phi)(1-\phi)\big)' \Bigg[\phi_k \sum_{l=1}^{N} \Bigg(\delta_l\phi_l(\delta_l - \delta_k) \prod_{\substack{n=1 \\ n\neq k,l}}^{N} (\delta_n - \delta_k) \Bigg) \\
&+ \sum_{m=1}^{N} \Bigg(\phi_m\delta_k\phi_k(\delta_k - \delta_m) \prod_{\substack{n=1 \\ n\neq k,m}}^{N} (\delta_n - \delta_k) \Bigg) \Bigg] \Bigg\} \big(V(\phi)(1-\phi)\big)^{N-1} \\
=& \Big\{ -\delta_k\phi_k V(\phi)(1-\phi) + \delta_k\phi_k\big(V(\phi)(1-\phi)\big)' - \phi_k\boldsymbol{\delta}^{\mathrm{T}}\Phi\big(V(\phi)(1-\phi)\big)' \\
&+ \phi_k\boldsymbol{\delta}^{\mathrm{T}}\Phi\big(V(\phi)(1-\phi)\big)' - \delta_k\phi_k\phi\big(V(\phi)(1-\phi)\big)' \Big\} \\
&\times \big(V(\phi)(1-\phi)\big)^{N-1} \prod_{\substack{l=1 \\ l\neq k}}^{N} (\delta_l - \delta_k),
\end{aligned}$$

from which (3.12) can be read off immediately. ∎

THEOREM 3.3. *If* $\varrho_1 = \cdots = \varrho_N = \varrho_s$, $\delta_1 > \delta_2 > \cdots > \delta_N$, *and* $\Phi \in \mathcal{D}^0_{\phi_{\max}}$, *then the system* (1.4) *is strictly hyperbolic; i.e., the Jacobian* $\boldsymbol{\mathcal{J}}_{\mathbf{f}^M}(\Phi)$ *has* N *distinct real eigenvalues.*

Proof. From (3.12) we see that

$$P(\gamma^k) = C_k\big(V(\phi)\big)^{N-1}(1-\phi)^N \prod_{\substack{m=1\\ m\neq k}}^{N} (\delta_m - \delta_k), \quad k = 1, \dots, N,$$

with $C_k := \delta_k\phi_k(V'(\phi)(1-\phi) - 2V(\phi))$. Since $C_1, \dots, C_N < 0$ on $\mathcal{D}^0_{\phi_{\max}}$ due to (2.19), we have

$$\operatorname{sgn}\big(P(\gamma^k)\big) = -\operatorname{sgn}\left(\prod_{\substack{m=1\\ m\neq k}}^{N} (\delta_m - \delta_k)\right) = -\operatorname{sgn}\left(\prod_{m=k+1}^{N} (\delta_m - \delta_k)\right) = (-1)^{N-k+1}.$$

Consequently, we have shown that $\operatorname{sgn}(P(\gamma^i)) = (-1)^{N+1-i}$ for $i = 1, \dots, N$. Whether N is even or odd, we have $P(\lambda) \to \infty$ as $\lambda \to -\infty$ and $P(\gamma^N) < 0$. In view of $\gamma^N < \gamma^{N-1} < \cdots < \gamma^1$ and since $P(\gamma^N) < 0$, there exists a number $\lambda_N < \gamma^N$ with $P(\lambda_N) = 0$. Furthermore, $\operatorname{sgn}(P(\gamma^i)) = (-1)^{N+1-i}$ implies that there exist $N-1$ numbers $\lambda_i \in (\gamma^{i+1}, \gamma^i)$, $i = 1, \dots, N-1$, with $P(\lambda_i) = 0$. This shows that $P(\lambda) = \det(\mathbf{J} - \lambda\mathbf{I})$ has N roots $\lambda_1, \dots, \lambda_N$ satisfying

$$\lambda_N < \gamma^N < \lambda_{N-1} < \gamma^{N-1} < \cdots < \lambda_2 < \gamma^2 < \lambda_1 < \gamma^1. \tag{3.14}$$

Thus the system (1.4) is strictly hyperbolic for all $\Phi \in \mathcal{D}^0_{\phi_{\max}}$, and Theorem 3.3 is proved. ∎

The statement of Theorem 3.3 can still be improved. In fact, it is desirable to have lower and upper bounds for all eigenvalues of $\boldsymbol{\mathcal{J}}_{\mathbf{f}^M}(\Phi)$. However, in (3.14) a lower bound for the eigenvalue λ_N of $\mathbf{J}$ is still lacking. The following theorem shows that by evaluating $P(\lambda)$ at a suitable number $\gamma^\infty < \gamma^1$ it is indeed possible to provide that bound.

THEOREM 3.4. *Define* $\gamma^\infty := -2\boldsymbol{\delta}^{\mathrm{T}}\Phi V(\phi)(1-\phi) + (V(\phi)(1-\phi))'(\boldsymbol{\delta}^{\mathrm{T}}\Phi + \phi)$. *Then, under the conditions of Theorem* 3.3, *the eigenvalues* $\nu_1(\Phi), \dots, \nu_N(\Phi)$ *of* $\boldsymbol{\mathcal{J}}_{\mathbf{f}^M}(\Phi)$ *satisfy*

$$\nu_i(\Phi) \in \big(\mu\bar{\varrho}_s V(\phi)(1-\phi)(\delta_i - \boldsymbol{\delta}^{\mathrm{T}}\Phi), \mu\bar{\varrho}_s V(\phi)(1-\phi)(\delta_{i+1} - \boldsymbol{\delta}^{\mathrm{T}}\Phi)\big), \quad i = 1, \dots, N-1, \tag{3.15}$$

$$\nu_N(\Phi) \in \big(\mu\bar{\varrho}_s V(\phi)(1-\phi)(\delta_N - \boldsymbol{\delta}^{\mathrm{T}}\Phi), \mu\bar{\varrho}_s\gamma^\infty\big). \tag{3.16}$$

Proof. We first evaluate $P(\lambda)$ assuming that $\delta(\lambda) < 0$. Moreover, to estimate the factor in curled brackets in the second equation of (3.13), we use $(V(\phi)(1-\phi))'/V(\phi)(1-\phi) < 0$ to justify deleting $-\delta_m$ and replacing δ_l^2 by δ_l in the last sum. Furthermore, we use $1/(\delta_m - \delta(\gamma^\infty)) < -1/\delta(\gamma^\infty)$ in several instances, which leads to

$$\begin{aligned}
&1 + \sum_{m=1}^{N} \frac{\phi_m}{\delta_m - \delta(\lambda)}\left[-\delta_m + \frac{(V(\phi)(1-\phi))'}{V(\phi)(1-\phi)}\left(\delta_m - \boldsymbol{\delta}^{\mathrm{T}}\Phi + \sum_{l=1}^{N} \frac{\delta_l\phi_l(\delta_l - \delta_m)}{\delta_l - \delta(\lambda)}\right)\right] \\
&\geq 1 - \frac{\boldsymbol{\delta}^{\mathrm{T}}\Phi}{\delta(\lambda)}\left(\frac{(V(\phi)(1-\phi))'}{V(\phi)(1-\phi)} - 1\right) \\
&\quad + \frac{(V(\phi)(1-\phi))'}{V(\phi)(1-\phi)}\left(\frac{\phi}{\delta(\lambda)^2}\sum_{l=1}^{N}\delta_l\phi_l - \boldsymbol{\delta}^{\mathrm{T}}\Phi\sum_{m=1}^{N}\frac{\phi_m}{\delta_m - \delta(\lambda)}\right).
\end{aligned}$$

If we delete the last sum, the left-hand part of this inequality will remain positive whenever

$$\delta^2(\lambda) + \delta(\lambda)\boldsymbol{\delta}^{\mathrm{T}}\Phi\left[1 - \frac{(V(\phi)(1-\phi))'}{V(\phi)(1-\phi)}\right] + \boldsymbol{\delta}^{\mathrm{T}}\Phi\phi\frac{(V(\phi)(1-\phi))'}{V(\phi)(1-\phi)} > 0.$$

This can be achieved by letting $\lambda = \gamma^\infty$ such that

$$\delta(\gamma^\infty) = \boldsymbol{\delta}^{\mathrm{T}}\Phi\left[\frac{(V(\phi)(1-\phi))'}{V(\phi)(1-\phi)} - 1\right] + \frac{(V(\phi)(1-\phi))'}{V(\phi)(1-\phi)}\phi.$$

In fact, making obvious simplifications, we then obtain $\phi(\phi + \boldsymbol{\delta}^{\mathrm{T}}\Phi) > 0$, and the inequality is proved. Since $\gamma^\infty < \gamma^N$, $P(\gamma^N) < 0$, and $P(\gamma^\infty) > 0$, the smallest eigenvalue λ_N of $\mathbf{J}$ satisfies $\gamma^\infty < \lambda_N < \gamma^N$. Combining this with (3.14) and recalling that the eigenvalues ν_i of $\boldsymbol{\mathcal{J}}_{\mathbf{f}^{\mathrm{M}}}(\Phi)$ are given by $\nu_i = \mu\bar{\varrho}_{\mathrm{s}}\lambda_i$, $i = 1, \ldots, N$, we obtain the statement of Theorem 3.4. ∎

4. Properties of the diffusion matrix. Using

$$\frac{\partial}{\partial z}\left(\frac{\phi_i}{\phi}\right) = \frac{1}{\phi}\frac{\partial\phi_i}{\partial z} - \frac{\phi_i}{\phi^2}\left(\frac{\partial\phi_1}{\partial z} + \cdots + \frac{\partial\phi_N}{\partial z}\right) = \frac{1}{\phi}\left\{\frac{\partial\phi_i}{\partial z} - \frac{\phi_i}{\phi}\left(\frac{\partial\phi_1}{\partial z} + \cdots + \frac{\partial\phi_N}{\partial z}\right)\right\}$$

for $i = 1, \ldots, N$ and defining $W(\phi) := -\mu V(\phi)/(g\phi)$ and

(4.1)
$$\eta_{ij}(\Phi) := W(\phi)\left\{(1-\phi)\phi_i(\delta_i - \boldsymbol{\delta}^{\mathrm{T}}\Phi)\sigma_{\mathrm{e}}'(\phi) + \left[\delta_i\delta_{ij} - \delta_j\phi_i - \frac{\phi_i}{\phi}(\delta_i - \boldsymbol{\delta}^{\mathrm{T}}\Phi)\right]\sigma_{\mathrm{e}}(\phi)\right\}$$

for $i, j = 1, \ldots, N$, where $\delta_{ij} = 1$ if $i = j$ and $\delta_{ij} = 0$ otherwise, we get from (2.22)

$$a_i\left(\Phi, \frac{\partial\Phi}{\partial z}\right) = \eta_{i1}(\Phi)\frac{\partial\phi_1}{\partial z} + \cdots + \eta_{iN}(\Phi)\frac{\partial\phi_N}{\partial z}, \quad i = 1, \ldots, N. \tag{4.2}$$

Defining the matrix $\mathbf{A}(\Phi) := (\eta_{ij}(\Phi))_{1\le i,j\le N}$ and taking $\mathbf{f} = \mathbf{f}^{\mathrm{M}}$, we can rewrite (2.29) in the form (1.2). We show that the eigenvalues of $\mathbf{A}(\Phi)$ are positive and pairwise distinct on $\mathcal{D}^0_{\phi_{\max}}\backslash\mathcal{D}_{\phi_{\mathrm{c}}}$ by evaluating the characteristic polynomial in a fashion similar to section 3. To this end, we first provide an explicit expression for $S(\lambda) := \det(W(\phi)^{-1}\mathbf{A}(\Phi) - \lambda\mathbf{I})$.

LEMMA 4.1. *Let $\delta^*(\lambda) := \lambda/\sigma_{\mathrm{e}}(\phi)$. Then the polynomial $S(\lambda)$ is given by*

$$\begin{aligned} S(\lambda) = &\left\{\sigma_{\mathrm{e}}(\phi) + \sum_{m=1}^{N}\frac{\phi_m}{\delta_m - \delta^*(\lambda)}\left[-\delta_m\sigma_{\mathrm{e}}(\phi) + \left((1-\phi)\sigma_{\mathrm{e}}'(\phi) - \frac{\sigma_{\mathrm{e}}(\phi)}{\phi}\right)\right.\right. \\ &\left.\left.\times\left(\delta_m - \boldsymbol{\delta}^{\mathrm{T}}\Phi + \sum_{l=1}^{N}\frac{\phi_l\delta_l(\delta_l - \delta_m)}{\delta_l - \delta^*(\lambda)}\right)\right]\right\}\big(\sigma_{\mathrm{e}}(\phi)\big)^{N-1}\prod_{k=1}^{N}\big(\delta_k - \delta^*(\lambda)\big). \end{aligned} \tag{4.3}$$

Proof. We write $\eta_{ij}(\Phi)/W(\phi) = s^i_j\phi_i + s^i\delta_{ij}$ for $1 \le i, j \le N$, where we define

$$s^i := \sigma_{\mathrm{e}}(\phi)\delta_i, \quad s^i_j := (1-\phi)(\delta_i - \boldsymbol{\delta}^{\mathrm{T}}\Phi)\sigma_{\mathrm{e}}'(\phi) - \left(\delta_j + \frac{1}{\phi}(\delta_i - \boldsymbol{\delta}^{\mathrm{T}}\Phi)\right)\sigma_{\mathrm{e}}(\phi)$$

for $i,j=1,\dots,N$. Consequently, $S(\lambda)$ can be written as

$$S(\lambda)=\begin{vmatrix} s_1^1\phi_1+s^1-\lambda & s_2^1\phi_1 & \dots & s_N^1\phi_1 \\ s_1^2\phi_2 & s_2^2\phi_2+s^2-\lambda & \dots & s_N^2\phi_2 \\ \vdots & \vdots & \ddots & \vdots \\ s_1^N\phi_N & s_2^N\phi_N & \dots & s_N^N\phi_N+s^N-\lambda \end{vmatrix}.$$

Observe that the numbers s_j^i satisfy

$$s_j^i-s_k^i=-\sigma_{\rm e}(\phi)(\delta_j-\delta_k),\qquad s_i^j-s_i^k=(\delta_j-\delta_k)\left[(1-\phi)\sigma_{\rm e}'(\phi)-\frac{\sigma_{\rm e}(\phi)}{\phi}\right],\qquad i=1,\dots,N; \tag{4.4}$$

i.e., the right-hand parts of (4.4) do not depend on i. Therefore, we may introduce

$$s_{j,k}:=s_j^1-s_k^1=\cdots=s_j^N-s_k^N,\quad s^{j,k}:=s_1^j-s_1^k=\cdots=s_N^j-s_N^k,\quad j,k=1,\dots,N.$$

We can now easily provide an explicit expression for $S(\lambda)$ in terms of the s's, since the rules for the s's correspond to those for the γ's. Thus, replacing $V(\phi)(1-\phi)$ by $\sigma_{\rm e}(\phi)$, $(V(\phi)(1-\phi))'$ by $(1-\phi)\sigma_{\rm e}'(\phi)-\sigma_{\rm e}(\phi)/\phi$, $\delta(\lambda)$ by $\delta^*(\lambda)=\lambda/\sigma_{\rm e}(\phi)$, we obtain (4.3) by closely following the proofs of Lemma 3.1 and of (3.11) in Lemma 3.2. ∎

To localize the eigenvalues of $\mathbf{A}(\Phi)$, we need to evaluate $S(\lambda)$ at $\lambda=0$ and $\lambda=s^1,\dots,s^N$. Using the analogy between $P(\lambda)$ and $S(\lambda)$, we can easily prove the following lemma.

LEMMA 4.2. *The determinant of* $\mathbf{A}(\Phi)$ *is given by* $\det(\mathbf{A}(\Phi))=(W(\phi))^N S(0)$, *where*

$$S(0)=\delta_1\cdots\delta_N\big(\sigma_{\rm e}(\phi)\big)^{N-1}\sigma_{\rm e}'(\phi)\phi(1-\phi)^2\quad \text{for } 0\le\phi\le\phi_{\max} \text{ and } N\ge 2. \tag{4.5}$$

Moreover, for $k=1,\dots,N$ *we have*

$$S(s^k)=\phi_k\delta_k\left\{(1-\phi)\left[(1-\phi)\sigma_{\rm e}'(\phi)-\frac{\sigma_{\rm e}(\phi)}{\phi}\right]-\sigma_{\rm e}(\phi)\right\}\big(\sigma_{\rm e}(\phi)\big)^{N-1}\prod_{\substack{m=1\\ m\ne k}}^{N}(\delta_m-\delta_k). \tag{4.6}$$

Proof. We set $\lambda=\delta^*(\lambda)=0$ in (4.3). Then (4.5) follows from

$$\begin{aligned} S(0)=&\left\{\sigma_{\rm e}(\phi)+\sum_{m=1}^{N}\frac{\phi_m}{\delta_m}\left[-\delta_m\sigma_{\rm e}(\phi)+\left((1-\phi)\sigma_{\rm e}'(\phi)-\frac{\sigma_{\rm e}(\phi)}{\phi}\right)\right.\right.\\ &\left.\left.\times(\delta_m-\boldsymbol{\delta}^{\rm T}\Phi+\boldsymbol{\delta}^{\rm T}\Phi-\delta_m\phi)\right]\right\}\big(\sigma_{\rm e}(\phi)\big)^{N-1}\delta_1\cdots\delta_N\\ =&\left\{\sigma_{\rm e}(\phi)-\phi\sigma_{\rm e}(\phi)+(1-\phi)\phi\left((1-\phi)\sigma_{\rm e}'(\phi)-\frac{\sigma_{\rm e}(\phi)}{\phi}\right)\right\}\big(\sigma_{\rm e}(\phi)\big)^{N-1}\delta_1\cdots\delta_N. \end{aligned} \tag{4.7}$$

Equation (4.6) can then be derived by closely following the proof of (3.12) in Lemma 3.2. ∎

THEOREM 4.3. *Let* $G(\phi):=\phi(1-\phi)^2\sigma_{\rm e}'(\phi)-\sigma_{\rm e}(\phi)$, *and assume that* $V(\phi)\ne 0$ *for* $\phi<\phi_{\max}$ *and* $V(\phi)=0$ *otherwise. Then, for all* $\Phi\in\mathcal{D}^0_{\phi_{\max}}\backslash\mathcal{D}_{\phi_{\rm c}}$, *the matrix* $\mathbf{A}(\Phi)$ *has* N *distinct positive eigenvalues* $\Lambda_1,\dots,\Lambda_N$; *i.e., the system* (1.2) *is strictly parabolic on* $\mathcal{D}^0_{\phi_{\max}}\backslash\mathcal{D}_{\phi_{\rm c}}$. *Moreover, we have the following:*

(a) *If Φ is chosen such that $G(\phi) > 0$, then these eigenvalues satisfy*

$$\begin{aligned} 0 < W(\phi)\sigma_{\mathrm{e}}(\phi)\delta_N < \Lambda_N < W(\phi)\sigma_{\mathrm{e}}(\phi)\delta_{N-1} < \Lambda_{N-1} \\ < \cdots < W(\phi)\sigma_{\mathrm{e}}(\phi)\delta_1 < \Lambda_1 < W(\phi)\delta_1\phi(1-\phi)^2\sigma_{\mathrm{e}}'(\phi). \end{aligned} \tag{4.8}$$

(b) *At those points Φ where $G(\phi) < 0$, we have*

$$\begin{aligned} 0 < W(\phi)\delta_N\phi(1-\phi)^2\sigma_{\mathrm{e}}'(\phi) < \Lambda_N < W(\phi)\sigma_{\mathrm{e}}(\phi)\delta_N < \Lambda_{N-1} \\ < W(\phi)\sigma_{\mathrm{e}}(\phi)\delta_{N-1} < \cdots < \Lambda_1 < W(\phi)\sigma_{\mathrm{e}}(\phi)\delta_1. \end{aligned} \tag{4.9}$$

(c) *If $G(\phi) = 0$, then the eigenvalues are given by $\Lambda_i = W(\phi)\sigma_{\mathrm{e}}(\phi)\delta_i$ for $i = 1, \ldots, N$.*

Proof. Using the function $G(\phi)$, we can rewrite (4.6) as

$$S(s^k) = \frac{\phi_k}{\phi}\delta_k G(\phi)\big(\sigma_{\mathrm{e}}(\phi)\big)^{N-1} \prod_{\substack{m=1 \\ m\neq k}}^{N} (\delta_m - \delta_k), \quad k = 1, \ldots, N. \tag{4.10}$$

This implies

$$\begin{aligned} \operatorname{sgn}\big(S(s^k)\big) &= \operatorname{sgn}\big(G(\phi)\big) \cdot \operatorname{sgn}\left(\prod_{\substack{m=1 \\ m\neq k}}^{N} (\delta_m - \delta_k) \right) \\ &= (-1)^{N-k} \operatorname{sgn}\big(G(\phi)\big), \quad k = 1, \ldots, N. \end{aligned} \tag{4.11}$$

Recall first that, for $\phi > \phi_{\mathrm{c}}$ and due to $\delta_1 > \delta_2 > \cdots > \delta_N$, we have $0 < s^N < s^{N-1} < \cdots < s^1$. If $\operatorname{sgn}(G(\phi)) = 1$, then $S(s^N) > 0$, $S(s^{N-1}) < 0$, and so on, until we obtain $S(s^2) > 0$ and $S(s^1) < 0$ if N is even and $S(s^2) < 0$ and $S(s^1) > 0$ if N is odd. Thus there exist $N - 1$ values

$$0 < s^N < \lambda_N < s^{N-1} < \lambda_{N-1} < s^{N-2} < \cdots < \lambda_3 < s^2 < \lambda_2 < s^1 < \lambda_1 \tag{4.12}$$

with $S(\lambda_2) = \cdots = S(\lambda_N) = 0$. Moreover, $S(\lambda) \to \infty$ for $\lambda \to \infty$ if N is even and $S(\lambda) \to -\infty$ if N is odd. Thus there exists an Nth number $\lambda_1 > s^1$ with $S(\lambda_1) = 0$. Since the determinant of a matrix is the product of its eigenvalues, which are all positive here, (4.7) implies

$$\begin{aligned} \lambda_1 = \frac{S(0)}{\lambda_2 \cdots \lambda_N} < \frac{S(0)}{s^2 \cdots s^N} &= \frac{\phi(1-\phi)^2\sigma_{\mathrm{e}}'(\phi)(\sigma_{\mathrm{e}}(\phi))^{N-1}\delta_1 \cdots \delta_N}{\delta_2 \cdots \delta_N (\sigma_{\mathrm{e}}(\phi))^{N-1}} \\ &= \delta_1\phi(1-\phi)^2\sigma_{\mathrm{e}}'(\phi). \end{aligned} \tag{4.13}$$

If $\operatorname{sgn}(G(\phi)) = -1$, then $S(s^N) < 0$, $S(s^{N-1}) > 0$, and so on, and $S(s^2) < 0$, $S(s^1) > 0$ if N is even, and $S(s^2) > 0$, $S(s^1) < 0$ if N is odd. This means that we have $N - 1$ values

$$s^N < \lambda_{N-1} < s^{N-1} < \lambda_{N-2} < s^{N-2} < \cdots < \lambda_1 < s^1 \tag{4.14}$$

with $S(\lambda_1) = \cdots = S(\lambda_{N-1}) = 0$. Since $S(s^N) < 0$ but $S(0) > 0$ due to Lemma 4.2, there exists an Nth value $\lambda_N \in (0, s^N)$ satisfying $S(\lambda_N) = 0$, and we have

$$\begin{aligned} \lambda_N = \frac{S(0)}{\lambda_1 \cdots \lambda_{N-1}} > \frac{S(0)}{s^1 \cdots s^{N-1}} &= \frac{\phi(1-\phi)^2\sigma_{\mathrm{e}}'(\phi)(\sigma_{\mathrm{e}}(\phi))^{N-1}\delta_1 \cdots \delta_N}{\delta_1 \cdots \delta_{N-1} (\sigma_{\mathrm{e}}(\phi))^{N-1}} \\ &= \delta_N\phi(1-\phi)^2\sigma_{\mathrm{e}}'(\phi). \end{aligned} \tag{4.15}$$

The eigenvalues of $\mathbf{A}(\Phi)$ are given by $\Lambda_i = W(\phi)\lambda_i$, $i = 1, \ldots, N$. Thus, parts (a) and (b) of Theorem 4.3 follow from (4.12)–(4.15). Part (c) is the common limit for $G(\phi) \uparrow 0$ and $G(\phi) \downarrow 0$. □

Since the eigenvalues $\Lambda_1, \ldots, \Lambda_N$ are positive independent of the sign of $G(\phi)$, we see that the system (1.2) is strictly parabolic for all Φ satisfying $\phi_c < \phi < 1$, although, due to the properties of σ_e and W, at least $N - 1$ of these eigenvalues approach zero as $\phi \downarrow \phi_c$ or $\phi \uparrow \phi_{max}$.

5. Strongly degenerate parabolic problems. We have demonstrated that polydisperse sedimentation models taking into account compression effects give rise to strongly degenerate parabolic (also known as mixed hyperbolic-parabolic) systems of PDEs. The general theory of *uniformly parabolic* systems is an old subject and is by now well developed; see [42, 63, 104]. One can consult [100] for some special uniformly parabolic systems, as well as [36, 58, 85] for some results on parabolic systems with weaker parabolicity conditions. The general mathematical theory of *hyperbolic* systems is also fairly well developed (at least in one spatial dimension); see, for example, [32] and the references therein. On the other hand, to date there exists no general theory for *strongly degenerate parabolic* systems. However, the mathematical theory for *scalar* strongly degenerate parabolic equations has advanced significantly in the last few years. It is well known that nonlinear degenerate parabolic equations exhibit "hyperbolic phenomena" like finite speed of propagation or the appearance of interfaces. These effects are consequences of the partial loss of parabolicity. *Strongly* degenerate parabolic equations (e.g., those arising in the theory of sedimentation-consolidation processes) exhibit even more novel hyperbolic features such as the appearance of shock waves, loss of uniqueness, and the need for entropy conditions. Recall that a simple example of a strongly degenerate equation is a hyperbolic equation. Hence, strongly degenerate parabolic equations will in general possess discontinuous (weak) solutions. Moreover, discontinuous solutions are not uniquely determined by their initial (and boundary) data. In fact, an additional condition—the entropy condition—is needed to single out the physically relevant weak solution of the problem.

An entropy condition for strongly degenerate parabolic equations was first proposed in [118], which also established existence of an entropy solution by passing to the limit in a parabolic regularization. In the one-dimensional case, uniqueness of the entropy solution was proved in [119, 120]; see also [6, 7, 8]. Uniqueness of entropy solutions for multidimensional equations was obtained in the recent work [28] for a particular homogeneous boundary value problem. Extensions of this uniqueness result to the initial value problem can be found in [61, 62] for bounded entropy solutions (of more general equations). Uniqueness for unbounded entropy solutions and kinetic solutions is studied in [30] and [31], respectively. The inhomogeneous Dirichlet boundary value problem is treated in [72]. Some other boundary value problems arising in the theory of sedimentation-consolidation processes are studied in [17, 21, 25]. Weakly coupled systems of (strongly) degenerate parabolic equations are treated in [57].

Following up the recent development of a well-posedness theory for scalar strongly degenerate parabolic equations, there has also been a lot of activity on the design and analysis of numerical methods for such equations. Most of this activity can be seen as natural extensions of ideas and techniques from the hyperbolic numerical literature. Let us here mention the studies on monotone finite difference schemes [45], operator splitting methods (see [44] for an overview), finite volume schemes [46, 80], central finite difference schemes [64], the local discontinuous Galerkin method [33], and BGK

schemes [2, 12]. Numerical methods for parabolic systems (with weak degeneracy) are studied and analyzed in [60, 68]. Applications of operator splitting methods and finite difference schemes to scalar sedimentation-consolidation models can be found in [18] and [20], respectively.

In the next section, we will present and apply certain numerical schemes for systems of strongly degenerate parabolic equations. Except for [2], the available numerical literature has so far dealt with *scalar* strongly degenerate parabolic equations. Let us add that the generality in [2] is such that it does not include systems of the form considered in the present paper.

6. Numerical results. The Kurganov–Tadmor (KT) scheme [64] can be regarded as a refinement of the essentially nonoscillatory Nessyahu–Tadmor scheme [77], where the improvement is based on local estimates of the propagation velocities of the Riemann fan emerging from the cell boundaries during each time step. Thus, the accuracy of the resulting scheme depends on how accurately the eigenvalues of the Jacobian of the flux vector are determined. Since only for small systems can these eigenvalues be determined exactly, it is important for large N that sharp estimates can be obtained with low computational effort. The analysis of section 3 indeed provides sharp estimates for the first-order system of equations. Given the importance of these analytical results for the KT scheme, we give in what follows a rather compressed but complete description of this scheme. A general introduction to central schemes for systems of conservation laws is given in [103].

6.1. General difference scheme. Consider the computational domain $Q_T := [0,1] \times [0,T]$ and a rectangular grid defined by $z_j := j\Delta z$, $j = 0, \dots, J$, where J is an even integer and $\Delta z := 1/J$ is the width of a half-cell, and $t_n := n\Delta t$, $n = 0, \dots, \mathcal{N}$, where $\Delta t := T/\mathcal{N}$, $\mathcal{N} \in \mathbb{N}$, and $\lambda := \Delta t/(2\Delta z)$ is the fixed mesh-size ratio. (Thus, all grid-point indices are integers.) The (approximate) cell average of ϕ_i, $i = 1, \dots, N$, with respect to the cell $[z_j, z_{j+2}]$ at time t_n is denoted by $\bar\phi^n_{i,j}$, and we define $\bar\Phi^n_j := (\bar\phi^n_{1,j}, \dots, \bar\phi^n_{N,j})^{\mathrm{T}}$, $j = 1, 3, \dots, J-1$, $n = 0, 1, \dots, \mathcal{N}$. We assume that at time $t = t_n$, $n = 0, 1, \dots, \mathcal{N}-1$, the vector $\bar\Phi^n_j$ either has been calculated from the previous time step (for $n \ge 1$) or is given by the discretization of the initial condition,

$$\bar\phi^0_{i,j} := \frac{1}{2\Delta z} \int_{z_{j-1}}^{z_{j+1}} \phi^0_i(\zeta)\, d\zeta, \quad j = 1, 3, \dots, J-1, \quad i = 1, \dots, N.$$

For the interior cells, the general scheme ("interior scheme") is of the type

$$\bar\Phi^{n+1}_j = \bar\Phi^n_j - \lambda(\mathbf{h}^n_{j+1} - \mathbf{h}^n_{j-1}) + \lambda(\mathbf{p}^n_{j+1} - \mathbf{p}^n_{j-1}), \qquad \begin{matrix} j = 3, 5, \dots, J-3, \\ n = 0, \dots, \mathcal{N}-1, \end{matrix} \tag{6.1}$$

where $\mathbf{h}^n_{j\pm1}$ and $\mathbf{p}^n_{j\pm1}$ are approximations of the "hyperbolic" and "parabolic" fluxes $\mathbf{f}^{\mathrm{M}}$ and $\mathbf{a}$, respectively, through the boundaries of cell $I_j := [z_{j-1}, z_{j+1}]$ at time t_n. The detailed computation of these fluxes from the solution values at time t_n is described in section 6.2.

While the interior scheme (6.1) approximates the field equation (1.2), the boundary conditions (2.31) are discretized by setting $\mathbf{h}^n_0 - \mathbf{p}^n_0 = 0$ and $\mathbf{h}^n_J - \mathbf{p}^n_J = 0$ for $n = 0, \dots, \mathcal{N}-1$. Inserting this into (6.1), where we set $j = 1$ and $j = J-1$, we obtain the following "boundary scheme":

$$\begin{gathered} \bar\Phi^{n+1}_1 = \bar\Phi^n_1 - \lambda\mathbf{h}^n_2 + \lambda\mathbf{p}^n_2, \qquad \bar\Phi^{n+1}_{J-1} = \bar\Phi^n_{J-1} + \lambda\mathbf{h}^n_{J-2} - \lambda\mathbf{p}^n_{J-2}, \\ n = 0, \dots, \mathcal{N}-1. \end{gathered} \tag{6.2}$$

The extension of the CFL stability condition for the explicit KT scheme stated in [64] for scalar equations to the present case of a strongly degenerate parabolic-hyperbolic problem reads

$$\frac{\Delta t}{\Delta z}\max_{\mathcal{D}_{\phi_{\max}}}\rho\big(\boldsymbol{\mathcal{J}}_{\mathbf{f}}(\Phi)\big)+\frac{\Delta t}{2\Delta z^2}\max_{\mathcal{D}_{\phi_{\max}}}\rho\big(\mathbf{A}(\Phi)\big)\le\frac{1}{4}, \tag{6.3}$$

where $\rho(\cdot)$ denotes the spectral radius. We view (6.3) as a *necessary* condition for the present explicit KT scheme to produce a physically relevant numerical result, and we emphasize that no rigorous convergence result is associated with (6.3). For that matter, an existence and uniqueness theory for the system (1.1) is still lacking.

6.2. Computation of the numerical fluxes. Given the vectors $\bar\Phi_j^n$, $j=1,3,\dots,J-1$, we calculate a piecewise linear reconstruction of the solution values at time t_n by determining the slope vector $\Phi_j'=(\phi_{1,j}',\dots,\phi_{N,j}')^{\mathrm{T}}$, $j=1,3,\dots,J-1$, whose components are defined by

$$\phi_{i,j}':=\begin{cases}0 & \text{for } j=1 \text{ and } j=J-1,\\ \mathrm{MM}\big(\theta(\bar\phi_{i,j}^n-\bar\phi_{i,j-2}^n),(\bar\phi_{i,j+2}^n-\bar\phi_{i,j-2}^n)/2,\\ \qquad\qquad \theta(\bar\phi_{i,j+2}^n-\bar\phi_{i,j}^n)\big) & \text{for } j=3,5,\dots,J-3\end{cases}$$

for $i=1,\dots,N$. Here $\mathrm{MM}(\cdot,\cdot,\cdot)$ is the minmod function given by $\mathrm{MM}(a,b,c)=\min(a,b,c)$ if $a,b,c>0$, $\mathrm{MM}(a,b,c)=\max(a,b,c)$ if $a,b,c<0$, and $\mathrm{MM}(a,b,c)=0$ otherwise. The extrapolated values of Φ at the cell boundaries z_j, $j=2,4,\dots,J-2$, are then given by

$$\Phi_j^{\mp}:=\bar\Phi_{j\mp1}^n\pm\frac{1}{2}\Phi_{j\mp1}',\qquad j=2,4,\dots,J-2,$$

and are used to calculate the local speeds of propagation

$$a_j^n:=\max\left\{\rho\left(\boldsymbol{\mathcal{J}}_{\mathbf{f}}(\Phi_j^-)\right),\rho\left(\boldsymbol{\mathcal{J}}_{\mathbf{f}}(\Phi_j^+)\right)\right\},\quad j=2,4,\dots,J-2. \tag{6.4}$$

Of course, it is feasible only for small N to use exact eigenvalues here. However, the analysis of section 3 provides estimates of the eigenvalues that can be used here (see section 6.3). Observe that, for each cell I_j, the solution of (1.4) with the piecewise linear initial data defined by $\bar\Phi_j^n$ and the slope vectors Φ_j' remains smooth for $t_n\le t\le t_{n+1}$ in the subinterval $[z_{j-1}+a_{j-1}^n\Delta t,z_{j+1}-a_{j+1}^n\Delta t]$ for $j=1,\dots,J$. Equipped with the numbers a_j^n and the vectors Φ_j', we next calculate the following vectors, which represent the parts of the cell averages pertaining to the left and right half-cells adjacent to $z=z_j$ that are mapped onto a smooth solution:

$$\Phi_{j,\mathrm{L}}^n:=\bar\Phi_{j-1}^n+\left(\frac{1}{2}-\lambda a_j^n\right)\Phi_{j-1}',\qquad \Phi_{j,\mathrm{R}}^n:=\bar\Phi_{j+1}^n-\left(\frac{1}{2}-\lambda a_j^n\right)\Phi_{j+1}'$$

for $j=2,4,\dots,J-2$. The vectors $\Phi_{j,\mathrm{L}}^n$ and $\Phi_{j,\mathrm{R}}^n$ are used to calculate the flux slope vectors

$$\mathbf{f}'(\Phi_{j,c}^n)=\big(f_1'(\Phi_{j,c}^n),\dots,f_N'(\Phi_{j,c}^n)\big)^{\mathrm{T}},\quad c=\mathrm{L},\mathrm{R},\quad j=2,4,\dots,J-2,$$

whose components are defined by

$$f_i'(\Phi_{2,\mathrm{L}}^n)=f_i'(\Phi_{J-2,\mathrm{L}}^n)=0,\qquad f_i'(\Phi_{2,\mathrm{R}}^n)=f_i'(\Phi_{J-2,\mathrm{R}}^n)=0,$$

and

$$f_i'(\Phi_{j,c}^n) := \mathrm{MM}\Big(\theta\big(f_i(\Phi_{j,c}^n) - f_i(\Phi_{j-2,c}^n)\big), \big(f_i(\Phi_{j+2,c}^n) - f_i(\Phi_{j-2,c}^n)\big)/2, \theta\big(f_i(\Phi_{j+2,c}^n) - f_i(\Phi_{j,c}^n)\big)\Big)$$

for $c = \mathrm{L}, \mathrm{R}$, $i = 1, \ldots, N$, and $j = 4, 6, \ldots, J-4$. We then calculate the predictor solution values

$$\Phi_{j,c}^{n+1/2} := \Phi_{j,c}^n - \frac{\lambda}{2}\mathbf{f}'(\Phi_{j,c}^n), \quad c = \mathrm{L}, \mathrm{R}, \quad j = 2, 4, \ldots, J-2,$$

at which the flux vector $\mathbf{f}$ is evaluated in order to calculate the new approximate values $\bar{\Psi}_j^{n+1}$, $j = 2, 3, \ldots, J-1, J$, of the solution at time t_{n+1}, which are referred to a nonuniform grid as follows. For $j = 2, 4, \ldots, J-2$, approximate cell averages $\bar{\Psi}_j^{n+1}$ referring to the intervals $[z_j - a_j^n \Delta t, z_j + a_j^n \Delta t]$, $j = 2, 4, \ldots, J-2$, are calculated by

$$\bar{\Psi}_j^{n+1} = \frac{1}{2}\big(\bar{\Phi}_{j-1}^n + \bar{\Phi}_{j+1}^n\big) + \frac{1 - \lambda a_j^n}{4}\big(\Phi_{j-1}' - \Phi_{j+1}'\big) - \frac{1}{2a_j^n}\Big[\mathbf{f}\big(\Phi_{j,\mathrm{R}}^{n+1/2}\big) - \mathbf{f}\big(\Phi_{j,\mathrm{L}}^{n+1/2}\big)\Big],$$

while the second family of approximate cell averages $\bar{\Psi}_j^{n+1}$ refers to the nonuniform cells $[z_{j-1} + a_{j-1}^n \Delta, z_{j+1} - a_{j+1}^n \Delta t] \subset I_j$, $j = 3, 5, \ldots, J-3$, and is calculated by

$$\bar{\Psi}_j^{n+1} = \bar{\Phi}_j^n - \frac{\lambda}{2}\big(a_{j+1}^n - a_{j-1}^n\big)\Phi_j' - \frac{\lambda}{1 - \lambda(a_{j-1}^n + a_{j+1}^n)}\Big[\mathbf{f}\big(\Phi_{j+1,\mathrm{L}}^{n+1/2}\big) - \mathbf{f}\big(\Phi_{j-1,\mathrm{R}}^{n+1/2}\big)\Big].$$

Using both families of nonuniform approximate cell averages, we determine the vector of discrete derivatives $\Psi_j' = (\Psi_{1,j}', \ldots, \Psi_{N,j}')^{\mathrm{T}}$ for $j = 2, 4, \ldots, J-2$, setting $\Psi_2' = \Psi_{J-2}' = 0$ and

$$\Psi_{i,j}' = \frac{1}{\Delta z}\mathrm{MM}\left(\theta\frac{\bar{\Psi}_{i,j}^{n+1} - \bar{\Psi}_{i,j-1}^{n+1}}{1 + \lambda(a_j^n - a_{j-2}^n)}, \frac{\bar{\Psi}_{i,j+1}^{n+1} - \bar{\Psi}_{i,j-1}^{n+1}}{2 + \lambda(2a_j^n - a_{j-2}^n - a_{j+2}^n)}, \theta\frac{\bar{\Psi}_{i,j+1}^{n+1} - \bar{\Psi}_{i,j}^{n+1}}{1 + \lambda(a_j^n - a_{j+2}^n)}\right)$$

for $i = 1, \ldots, N$ and $j = 4, 6, \ldots, J-4$, where $\theta \in [0, 2]$ is a parameter. Finally, we can calculate the desired numerical flux vectors

$$\mathbf{h}_j^n = \frac{1}{2}\Big[\mathbf{f}\big(\Phi_{j,\mathrm{R}}^{n+1/2}\big) + \mathbf{f}\big(\Phi_{j,\mathrm{L}}^{n+1/2}\big)\Big] - \frac{a_j^n}{2}\big(\bar{\Phi}_{j+1}^n - \bar{\Phi}_{j-1}^n\big) + \frac{a_j^n(1 - \lambda a_j^n)}{4}\big(\Phi_{j-1}' + \Phi_{j+1}'\big) + \lambda\Delta z\big(a_j^n\big)^2\Psi_j', \quad j = 2, 4, \ldots, J-2.$$

For the diffusion part, we approximate $\partial\Phi/\partial z(z_j, t_n)$ by the slope vector

$$\widetilde{\Phi}_j' = (\tilde{\phi}_{1,j}', \ldots, \tilde{\phi}_{N,j}')^{\mathrm{T}}$$

defined by $(\bar{\phi}_{i,j+1}^n - \bar{\phi}_{i,j-1}^n)/(2\Delta z)$ for $j = 2, 4, \ldots, J-2$ and $i = 1, \ldots, N$. Using the diffusion vector $\mathbf{a}(\Phi, \partial\Phi/\partial z)$ given by (4.2), we can calculate the numerical diffusion vectors by

$$\mathbf{p}_j^n = \frac{1}{2}\Big[\mathbf{a}\big(\bar{\Phi}_{j-1}, \widetilde{\Phi}_j'\big) + \mathbf{a}\big(\bar{\Phi}_{j+1}, \widetilde{\Phi}_j'\big)\Big], \quad j = 2, 4, \ldots, J-2. \tag{6.5}$$

6.3. Application to the model of polydisperse sedimentation with compression. In the numerical examples, we consider the standard Richardson and Zaki [86] hindered settling factor

$$V(\phi) = \begin{cases} 0 & \text{for } \phi \le 0 \text{ and } \phi \ge \phi_{\max}, \\ (1-\phi)^{n-2},\ n > 2, & \text{otherwise} \end{cases} \tag{6.6}$$

and the widely used power-law effective solid-stress formula

$$\sigma_{\mathrm{e}}(\phi) = \begin{cases} 0 & \text{for } \phi \le \phi_{\mathrm{c}}, \\ \sigma_0\big((\phi/\phi_{\mathrm{c}})^k - 1\big) & \text{for } \phi > \phi_{\mathrm{c}}, \end{cases} \quad \text{i.e.,} \quad \sigma_{\mathrm{e}}'(\phi) = \begin{cases} 0 & \text{for } \phi < \phi_{\mathrm{c}}, \\ (\sigma_0/\phi_{\mathrm{c}}^k) k \phi^{k-1} & \text{for } \phi > \phi_{\mathrm{c}}, \end{cases} \tag{6.7}$$

with parameters $\sigma_0 > 0$ and $k \ge 1$. Values of σ_0, ϕ_{c}, and k for real materials are given in [16, 105].

For our choice of $V(\phi)$ and under the mild assumption $\phi_{\max} > 1/n$, we may significantly sharpen the upper bound for the eigenvalues of $\boldsymbol{\mathcal{J}}_{\mathbf{f}^{\mathrm{M}}}(\Phi)$ compared with the bound given by Theorem 3.4.

LEMMA 6.1. *For the hindered settling function* (6.6) *and* $\Phi \in \mathcal{D}^0_{1/n}$, *i.e.,* $\phi < 1/n < \phi_{\max}$, *the eigenvalues* $\nu_1(\Phi)$ *to* $\nu_N(\Phi)$ *of* $\boldsymbol{\mathcal{J}}_{\mathbf{f}^{\mathrm{M}}}(\Phi)$ *satisfy* (3.15) *and*

$$\nu_N(\Phi) \in \big(\mu\bar{\varrho}_{\mathrm{s}} V(\phi)(1-\phi)(\delta_N - \boldsymbol{\delta}^{\mathrm{T}}\Phi), -\mu\bar{\varrho}_{\mathrm{s}} V(\phi)(1-\phi)\boldsymbol{\delta}^{\mathrm{T}}\Phi\big). \tag{6.8}$$

Proof. We set $\widetilde{\gamma}^{\infty} := -V(\phi)(1-\phi)\boldsymbol{\delta}^{\mathrm{T}}\Phi$ such that $\delta(\widetilde{\gamma}^{\infty}) = 0$. Using (3.11), we get

$$\begin{aligned} P(\widetilde{\gamma}^{\infty}) &= \left\{ V(\phi)(1-\phi) + \sum_{m=1}^{N} \frac{\phi_m}{\delta_m} \Big[-\delta_m V(\phi)(1-\phi) + \big(V(\phi)(1-\phi)\big)'(1-\phi)\delta_m \Big] \right\} \\ &\qquad \times \big(V(\phi)(1-\phi)\big)^{N-1} \delta_1 \cdots \delta_N \\ &= \Big\{ V(\phi)(1-\phi) - \phi V(\phi)(1-\phi) + \big(V(\phi)(1-\phi)\big)'\phi(1-\phi) \Big\} \\ &\qquad \times \big(V(\phi)(1-\phi)\big)^{N-1} \delta_1 \cdots \delta_N \\ &= \Big\{ V(\phi)(1-\phi) + \big(V(\phi)(1-\phi)\big)'\phi \Big\} (1-\phi)^N \big(V(\phi)\big)^{N-1} \delta_1 \cdots \delta_N. \end{aligned}$$

For $V(\phi) = (1-\phi)^{n-2}$, the expression in curled brackets is given by

$$\begin{aligned} (1-\phi)^{n-1} - (n-1)(1-\phi)^{n-2}\phi &= (1-\phi)^{n-2}\big((1-\phi) - (n-1)\phi\big) \\ &= (1-\phi)^{n-2}(1-n\phi), \end{aligned}$$

which is positive if and only if $\phi < 1/n$. In this case we thus have $P(\widetilde{\gamma}^{\infty}) > 0$. Since $\widetilde{\gamma}^{\infty} < \gamma^N$, $P(\gamma^N) < 0$, and we have now shown that $P(\widetilde{\gamma}^{\infty}) > 0$, the smallest eigenvalue λ_N of $\mathbf{J}$ satisfies $\widetilde{\gamma}^{\infty} < \lambda_N < \gamma^N$, which implies the statement of the lemma. ∎

Wherever $\phi < 1/n$, Lemma 6.1 can be used to estimate the local speeds of propagation (6.4) in the numerical method since, for our choice of $V(\phi)$, we then have that $\rho(\boldsymbol{\mathcal{J}}_{\mathbf{f}}(\Phi)) \le \mu\bar{\varrho}_{\mathrm{s}}(1-\phi)^{n-1} \max\{\boldsymbol{\delta}^{\mathrm{T}}\Phi, 1 - \boldsymbol{\delta}^{\mathrm{T}}\Phi\}$. Similarly, the eigenvalue bounds of Theorem 4.3 can be utilized to estimate the term $\max \rho(\boldsymbol{\mathcal{J}}_{\mathbf{f}})$ required in the CFL condition (6.3), which limits the step size ratio.

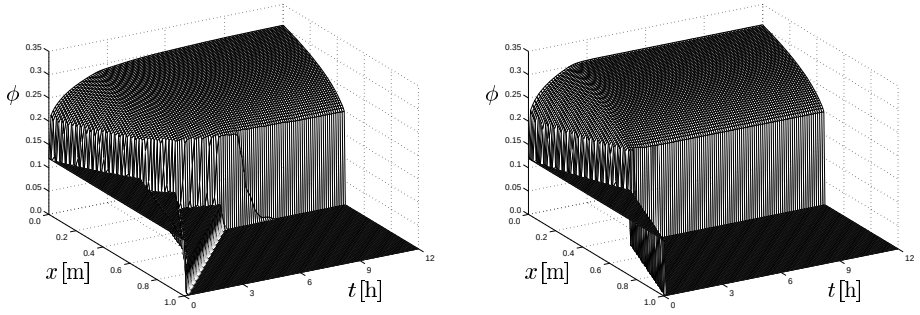

FIG. 1. *Simulations of the sedimentation-consolidation process of a tridisperse suspension (left) and a monodisperse suspension (right) using the same model functions $V(\phi)$ and $\sigma_e(\phi)$: plots of the (total) solids concentration ϕ.*

6.4. Numerical results. The numerical scheme is now employed to simulate settling processes of a tridisperse ($N = 3$) suspension forming compressible sediment. We consider here a (hypothetical) mixture described by the model functions (6.6) with $\phi_{\max} = 0.66$ and $n = 4.7$ (see [94]) and (6.7) with $\sigma_0 = 180\,\mathrm{Pa}$, $\phi_c = 0.2$, and $k = 6$. The remaining parameters are $\mu_f = 10^{-3}\mathrm{Pa{\cdot}s}$ (the dynamic viscosity of water), $d_1 = 1.19 \times 10^{-5}\,\mathrm{m}$, $\bar{\varrho}_s = 1800\,\mathrm{kg/m^3}$, and $g = 9.81\,\mathrm{m/s^2}$.

6.4.1. Settling of a tridisperse suspension. We consider an initially homogeneous suspension with $d_2/d_1 = \sqrt{0.5}$ and $d_3/d_1 = 0.5$, such that $\boldsymbol{\delta} = (1, 0.5, 0.25)^{\mathrm{T}}$, and $\Phi^0 = (0.04, 0.04, 0.04)^{\mathrm{T}}$ in a vessel of height $L = 1\,\mathrm{m}$. For the simulation, we chose $J = 1000$ and $\lambda = 0.0008\,\mathrm{h/m}$. The left diagram of Figure 1 shows the total volumetric solids concentration $\phi = \phi_1 + \phi_2 + \phi_3$ as a function of z and t, while Figure 2 displays the corresponding concentrations of the individual species.

To make the numerical results comparable to those obtained from the two existing models for monodisperse flocculated suspensions and for polydisperse suspensions of rigid spheres, we show in the right diagram of Figure 1 a simulation of the settling of a monodisperse suspension with $\phi_0 = 0.12$, and in Figure 3 the simulation of a tridisperse suspension of rigid particles (forming a sediment without compressibility effects) having the same parameters as the previously discussed case but with $\sigma_0 = 0$. The simulation shown in Figure 3 was made with $\lambda = 0.35\,\mathrm{h/m}$ and $J = 8000$. Note that the visual grid used in all diagrams is much coarser than the computational grid.

6.4.2. Effect of a third particle species on the settling of a bidisperse suspension. To study the effect of the size of a third species on the separation of two other species, we first consider a bidisperse suspension having the parameters given above and $\boldsymbol{\delta}^{\mathrm{T}} = (1.0, 0.5)$. The initial concentration is $\Phi^0 = (0.06, 0.06)^{\mathrm{T}}$. Other parameters for this simulation (and that of Figure 5) are $\lambda = 0.0008\,\mathrm{s/m}$, $J = 600$, and $L = 1\,\mathrm{m}$. Figure 4 shows a simulation of the settling of this suspension.

Next, we add a third species to this bidisperse mixture. The corresponding numerical results are shown in Figure 5. The left and right columns correspond to the size parameters $\delta_3 = 0.25$ and $\delta_3 = 0.1$, respectively. The initial concentrations of the tridisperse mixture are $\Phi^0 = (0.06, 0.06, 0.015)^{\mathrm{T}}$.

6.5. Discussion of the numerical results. In the left plot of Figure 1, three distinct zones are formed by the downwards-propagating concentration discontinuities, and, as expected, the concentration ϕ in the sediment bed increases more slowly than

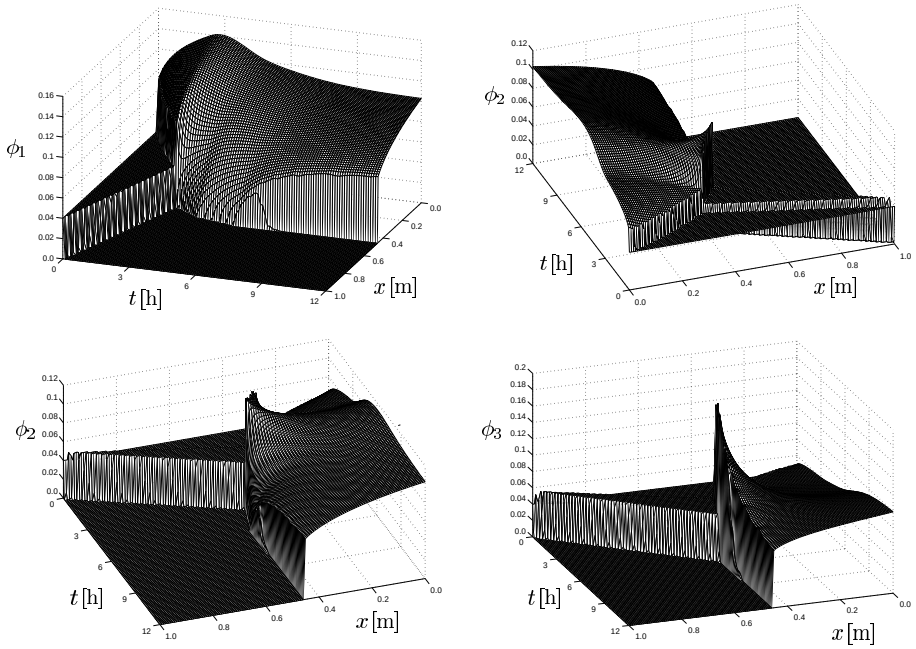

FIG. 2. *Simulation of the sedimentation-consolidation process of a tridisperse suspension: plots of the concentrations ϕ_1 of the largest (top left), ϕ_2 of the second-largest (top right and bottom left; two different views), and ϕ_3 of the smallest species (bottom right).*

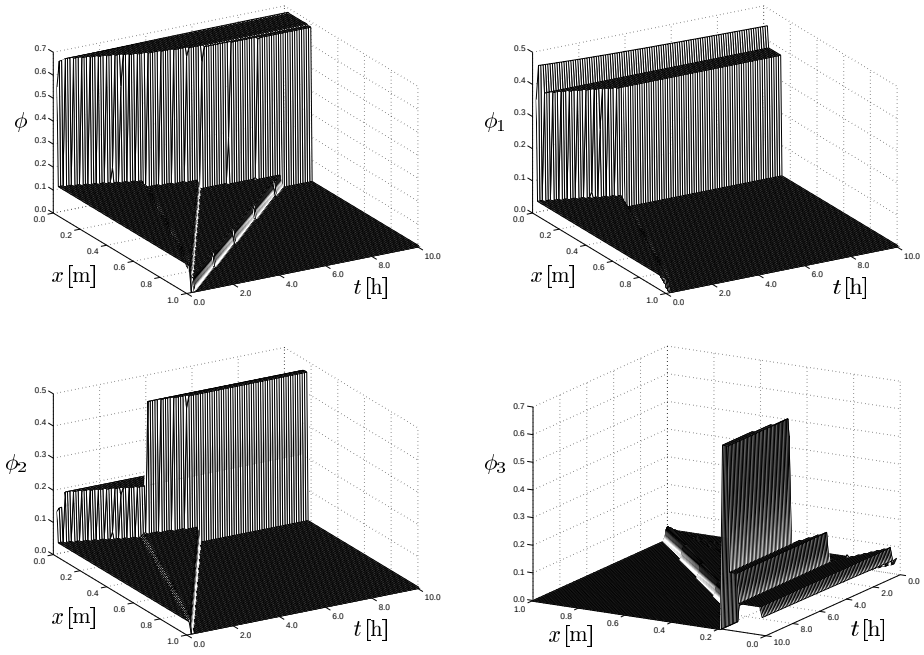

FIG. 3. *Simulation of the sedimentation of a tridisperse suspension of rigid particles (without compression, $\sigma_e \equiv 0$): plots of the cumulative concentration ϕ (top left) and the concentrations ϕ_1, ϕ_2, and ϕ_3 of the largest (top right), the second-largest (bottom left), and smallest species (bottom right).*

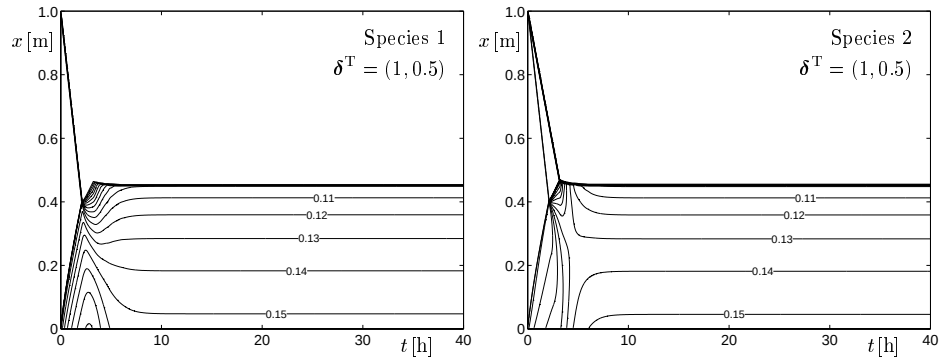

FIG. 4. *Simulation of the settling of an initially homogenous bidisperse suspension: iso-line of the concentrations ϕ_1 of the larger (left) and ϕ_2 of the smaller (right) species, corresponding to $\phi_{1,2} = 0, 0.01, 0.02, 0.03, \ldots$.*

in the monodisperse case. Comparing ϕ in the two tridisperse cases, we see that the zones formed in the first stages of sedimentation are still visible in the upper left plot of Figure 3, but have been entirely smoothed out in the left plot of Figure 1.

The two bottom plots of Figure 3 show the expected layering caused by differential sedimentation and the consequent enhancement of ϕ_2 and ϕ_3 above the lowest zone. Additional numerical examples illustrating the conventional model of sedimentation of suspensions of rigid spheres (when $\sigma_e = 0$) are given in [14, 19] (see also [48]). Figure 2 shows that the additional terms in the equation for suspensions forming compressible sediments result in the upward diffusion of the largest spheres and the downward diffusion of the smallest. Though these terms were expected to smooth the sharp boundaries found in suspensions of incompressible particles, the extent of the migration was unexpected.

The simulations described in (6.4.2) elucidate this phenomenon. We first simulated the sedimentation of an initially homogeneous bidisperse suspension and plotted the isolines of concentration. Figure 4 shows that these isolines ultimately have the same value for both species. This is a consequence of the assumption that $(\phi_i/\phi)\sigma_e(\phi)$ is the part of σ_e that acts on species i. For particles of equal density, and if we assume $V(\phi) > 0$, then the one-dimensional equilibrium form of (2.20) is

$$\bar{\varrho}_s(1-\phi) + \frac{\sigma_e(\phi)}{g\phi_i}\frac{d}{dz}\left(\frac{\phi_i}{\phi}\right) + \frac{1-\phi}{g\phi}\frac{d\sigma_e(\phi)}{dz} = 0, \quad i = 1, \ldots, N, \tag{6.9}$$

which can be rearranged to

$$\frac{d}{dz}\ln\left(\frac{\phi_i}{\phi}\right) = -\frac{1-\phi}{\sigma_e(\phi)}\left(\bar{\varrho}_s g\phi + \frac{d\sigma_e(\phi)}{dz}\right), \quad i = 1, \ldots, N. \tag{6.10}$$

From (3.53) of [27] with $u = 0$, or by setting $\phi_i = \phi$ in (6.9), we see that the expression in large parentheses is zero. Thus, ϕ_i/ϕ is constant and we have

$$\lim_{t\to\infty}\frac{\phi_i(z,t)}{\phi(z,t)} = \frac{\phi_i^0}{\phi_1^0 + \cdots + \phi_N^0}, \quad i = 1, \ldots, N. \tag{6.11}$$

The same phenomenon is also clear in Figure 5. Here the isolines of species 1 and 2 have the same ultimate values, while those of species 3 are proportional to its initial concentration.

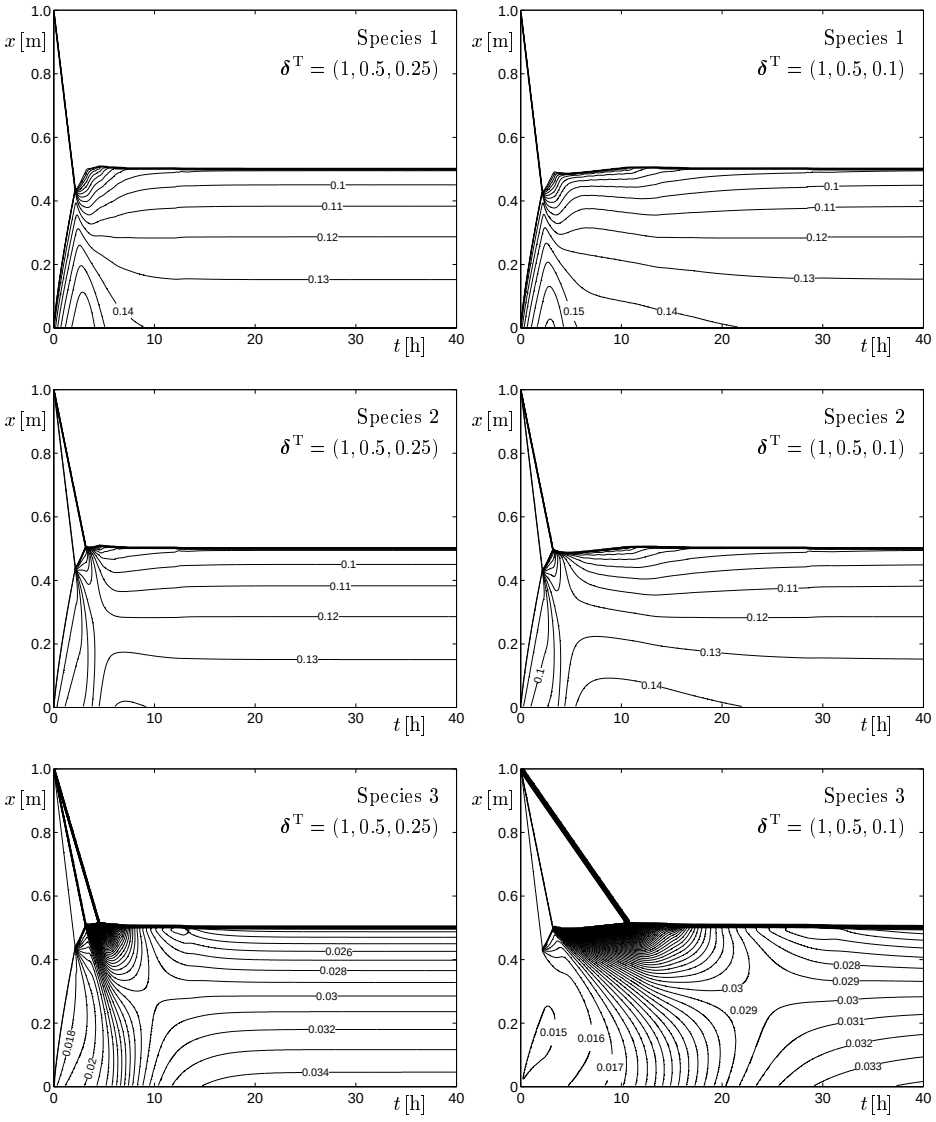

FIG. 5. *Simulations of the settling of tridisperse suspensions with different sizes of species* 3 *($d_3 = 0.5d_1$ in the left and $d_3 = 0.0.316d_1$ in the right column): iso-lines of the concentrations ϕ_1 of the larger (top) and ϕ_2 of the medium-sized (middle) species, corresponding to $\phi_{1,2} = 0, 0.01, 0.02, 0.03, \ldots$, and ϕ_3 of the smallest species (bottom) for $\phi_3 = 0, 0.001, 0.002, \ldots$.*

The complicated structures of the isolines at lower values of t arise from the resolution of the disparity between the segregation that occurs early in the sedimentation process and the ultimate uniformity with respect to species. The details of the process depend sensitively on the values of the terms in a_i. However, certain features are common.

We first consider a bidisperse suspension. When $\phi < \phi_{\mathrm{c}}$, the largest species settles most quickly and predominates in the lower region. In the consolidation phase ($\phi > \phi_{\mathrm{c}}$), the increase in ϕ tends to increase the concentration of both species in

the lower region. Figure 4 shows that species 1 reaches a concentration of 0.18 at the bottom while species 2 is still settling into the top (monodisperse) layer of the solids in compression. However, the larger particles diffuse into this layer, and the smaller particles diffuse out of it. This diffusion continues until the equilibrium state is reached.

In the tridisperse case shown in Figure 5, species 1 diffuses upward while species 2 diffuses both upward into the initially monodisperse upper layer of small particles and downward into the lower layer where large particles initially predominate. Species 3 diffuses downward from the top layer. In addition to reducing the final concentrations of the two larger species, the introduction of the smallest particles delays the evolution to the equilibrium state by introducing a segregated layer at the top of the suspension. In the example on the left, species 3 settles fairly quickly, and the change from segregated to uniform state occurs much earlier than in the example on the right, where species 3 settles very slowly. Further discussion of the phenomenon of sediment diffusivity seen in our simulations is provided in section 7.5.

7. Discussion.

7.1. Type analysis in several space dimensions. The type analysis confirms that the model is well-posed in that the one-dimensional system (1.2) is not of "general" type but has desirable algebraic properties. The analysis in sections 3 and 4 has been limited to one space dimension for notational convenience and since only in that case does the system (2.29), supplemented by the initial and boundary conditions (2.30) and (2.31), completely describe the sedimentation-consolidation process. In $D > 1$ space dimensions, not only system (2.23) for the concentrations of the solids species but also (2.24) and (2.25) for the motion of the mixture have to be solved. These equations are strongly coupled and probably will have to be solved alternately. Although, for $D > 1$, (2.23) no longer completely describes the sedimentation-consolidation process, this multidimensional system still is strongly degenerate parabolic-hyperbolic. To see this, consider first the case $\phi \le \phi_c$, for which the right-hand side of (2.23) vanishes. On the other hand, we recall that a D-dimensional $N \times N$ system of conservation laws

$$\frac{\partial \mathbf{u}}{\partial t} + \frac{\partial \boldsymbol{\varphi}_1(\mathbf{u})}{\partial x_1} + \cdots + \frac{\partial \boldsymbol{\varphi}_D(\mathbf{u})}{\partial x_D} = 0,$$

with $\mathbf{u} \in \mathcal{D} \subset \mathbb{R}^N$ and flux vectors $\boldsymbol{\varphi}_1, \ldots, \boldsymbol{\varphi}_D : \mathcal{D} \to \mathbb{R}^N$, is called hyperbolic if any linear combination $\boldsymbol{\mathcal{J}}(\boldsymbol{\beta}, \mathbf{u}) := \beta_1 \boldsymbol{\mathcal{J}}_{\boldsymbol{\varphi}_1}(\mathbf{u}) + \cdots + \beta_D \boldsymbol{\mathcal{J}}_{\boldsymbol{\varphi}_D}(\mathbf{u})$ of the Jacobians of the flux vectors is diagonalizable with real eigenvalues. The nonlinear fluxes $f_1^{\mathrm{M}}(\Phi), \ldots, f_N^{\mathrm{M}}(\Phi)$ in (2.23) are effective in the vertical direction of the z coordinate only. Considering $D = 3$ (the case $D = 2$ is analogous) and $\mathbf{q} = (q_x, q_y, q_z)^{\mathrm{T}}$, we obtain from (2.23) $\boldsymbol{\varphi}_1(\Phi) = q_x \Phi$, $\boldsymbol{\varphi}_2(\Phi) = q_y \Phi$, and $\boldsymbol{\varphi}_3(\Phi) = q_z \Phi + \mathbf{f}^{\mathrm{M}}(\Phi)$. Thus, the relevant linear combinations are $\boldsymbol{\mathcal{J}}(\boldsymbol{\beta}; \Phi) := (\beta_1 q_x + \beta_2 q_y + \beta_3 q_z)\mathbf{I} + \beta_3 \boldsymbol{\mathcal{J}}_{\mathbf{f}^{\mathrm{M}}}(\Phi)$, where $\boldsymbol{\mathcal{J}}_{\mathbf{f}^{\mathrm{M}}}(\Phi)$ is the Jacobian considered in section 3. Since $\boldsymbol{\mathcal{J}}_{\mathbf{f}^{\mathrm{M}}}(\Phi)$ has N pairwise-distinct eigenvalues and is thus diagonalizable, $\boldsymbol{\mathcal{J}}(\boldsymbol{\beta}; \Phi)$ is also diagonalizable with real eigenvalues, and (2.23) is therefore hyperbolic for $\phi \le \phi_c$. Of course, this statement is true under the same conditions as in the one-dimensional case, that is, for equal-density spheres and vectors $\Phi \in \mathcal{D}^0_{\phi_{\max}}$.

Next, we show that the system (2.23) is parabolic for $\phi > \phi_c$. More precisely, we show that it satisfies the classical definition of parabolicity in the sense of Petrovsky

[42, 49, 66, 104]. We do not state this condition in its most general form but limit the discussion to equations of the form

$$\frac{\partial u_i}{\partial t} + F_i(\mathbf{x}, t, \mathbf{u}, \nabla \mathbf{u}) = \sum_{m,n=1}^{D} \sum_{j=1}^{N} A_{ij}^{mn}(\mathbf{x}, t, \mathbf{u}) \frac{\partial^2 u_j}{\partial x_m \partial x_n}, \quad i = 1, \ldots, N. \tag{7.1}$$

Consider the matrix $\boldsymbol{\mathcal{A}}(\mathbf{x}, t, \mathbf{u})^{mn} := (A_{ij}^{mn})_{1 \le i,j \le N}$. Then (7.1) is called *parabolic in the sense of Petrovsky* (or simply *parabolic*) at a point $(\mathbf{x}, t, \mathbf{u}) \in Q_T \times \mathcal{D} \subset \mathbb{R}^D \times \mathbb{R}^+ \times \mathbb{R}^N$ if, for all vectors $\boldsymbol{\xi} = (\xi_1, \ldots, \xi_D)^{\mathrm{T}}$ with $|\boldsymbol{\xi}| = 1$, the roots $\lambda = \lambda(\mathbf{x}, t, \mathbf{u}, \boldsymbol{\xi})$ of $\det(\boldsymbol{\mathcal{A}}(\mathbf{x}, t, \mathbf{u}, \boldsymbol{\xi}) - \lambda \mathbf{I}) = 0$, where

$$\boldsymbol{\mathcal{A}}(\mathbf{x}, t, \mathbf{u}, \boldsymbol{\xi}) := \sum_{m,n=1}^{D} -\boldsymbol{\mathcal{A}}^{mn}(\mathbf{x}, t, \mathbf{u}) \xi_n \xi_m,$$

satisfy $\mathrm{Re}\,(\lambda(\mathbf{x}, t, \mathbf{u}, \boldsymbol{\xi})) < -\delta(\mathbf{x}, t, \mathbf{u})$ for a constant $\delta > 0$. We now consider the right-hand part of (2.25). From (4.1) and (4.2) we get $\mathbf{a}_i(\Phi, \nabla\Phi) = \eta_{i1}(\Phi)\nabla\phi_1 + \cdots + \eta_{iN}(\Phi)\nabla\phi_N$ and therefore

$$\begin{aligned} \nabla \cdot \mathbf{a}_i(\Phi, \nabla\Phi) &= \sum_{m=1}^{D} \sum_{j=1}^{N} \frac{\partial}{\partial x_m} \left(\eta_{ij}(\Phi) \frac{\partial \phi_j}{\partial x_m} \right) \\ &= \sum_{m=1}^{D} \sum_{j=1}^{N} \eta_{ij}(\Phi) \frac{\partial^2 \phi_j}{\partial x_m^2} + \sum_{m=1}^{D} \sum_{j=1}^{N} \frac{\partial \eta_{ij}(\Phi)}{\partial \phi_j} \left(\frac{\partial \phi_j}{\partial x_m} \right)^2. \end{aligned}$$

Defining

$$F_i(\mathbf{x}, t, \Phi, \nabla\Phi) := \nabla \cdot \left(\phi_i \mathbf{q} + f_i^{\mathrm{M}}(\Phi) \right) - \sum_{m=1}^{D} \sum_{j=1}^{N} \frac{\partial \eta_{ij}(\Phi)}{\partial \phi_j} \left(\frac{\partial\ \phi_j}{\partial x_m} \right)^2, \quad i = 1, \ldots, N,$$

we can rewrite (2.23) in the form (7.1). We then obtain $\boldsymbol{\mathcal{A}}^{mn}(\mathbf{x}, t, \Phi) = \mathbf{A}(\Phi)$ for all $1 \le m, n \le D$ if $m = n$, and $\boldsymbol{\mathcal{A}}^{mn}(\mathbf{x}, t, \Phi) = 0$ otherwise, where $\mathbf{A}(\Phi)$ was introduced in section 4. This implies $\boldsymbol{\mathcal{A}}(\mathbf{x}, t, \Phi, \boldsymbol{\xi}) = -\mathbf{A}(\Phi)$ for all $\boldsymbol{\xi} \in \mathbb{R}^D$ with $|\boldsymbol{\xi}| = 1$. From Theorem 4.3 we see that $\boldsymbol{\mathcal{A}}(\mathbf{x}, t, \Phi, \boldsymbol{\xi})$ has N distinct real eigenvalues $-\Lambda_1, \ldots, -\Lambda_N$ for $\Phi \in \mathcal{D}^0_{\phi_{\max}} \backslash \mathcal{D}_{\phi_c}$. This implies that the parabolicity condition $\mathrm{Re}\,(\lambda(\Phi, \boldsymbol{\xi})) < -\delta(\Phi)$ holds with $\delta(\Phi) = W(\phi)\delta_N \min\{\sigma_e(\phi), \phi(1-\phi)^2\sigma_e'(\phi)\}$. Thus, system (2.23) is parabolic on $\mathcal{D}^0_{\phi_{\max}} \backslash \mathcal{D}_{\phi_c}$, and we conclude that the hyperbolicity and parabolicity properties obtained in sections 3 and 4 remain valid in an arbitrary number of space dimensions.

7.2. Extension to particles with different densities. The model equations established in section 2 admit that the solids species differ in both size and density. The analysis of section 3 is valid for the case of equal-density particles only, while the matrix $\mathbf{A}(\Phi)$ is independent of the particle densities. In [22] it was demonstrated that different densities lead to hyperbolic-elliptic or (for $N \ge 3$) nonhyperbolic systems. Thus, it is tempting to conclude that the model framework of section 2 leads to systems having even more interesting properties (like a second-order parabolic system for $N = 2$ degenerating into a first-order hyperbolic-elliptic one). However, since particles of different densities consist of different materials, the assumption $\sigma_e(\Phi) = \sigma_e(\phi)$, stating that the effective stress depends only on the sediment porosity $1 - \phi$, is very unlikely to remain valid.

7.3. Physical explanation of Lemma 6.1. Recall that $f_i^{\mathrm{M}}(\Phi) = \phi_i v_i$, where v_i is the phase velocity of species i, that is, the settling velocity of a particle of species i. In view of (3.1), Theorem 3.4 states that the eigenvalues ν_1 to ν_{N-1} of $\boldsymbol{\mathcal{J}}_{\mathbf{f}^{\mathrm{M}}}(\Phi)$ satisfy $v_i \le \nu_i \le v_{i+1}$; i.e., the propagation of the characteristic information associated with the eigenvalue ν_i is bounded by the physical velocities of particles of species i and $i+1$ for $i = 1, \dots, N-1$. The upper bound on ν_N given by the parameter γ^∞ of Theorem 3.4, which is valid for any admissible hindered settling function $V(\phi)$, has no obvious physical interpretation, but Theorem 3.4 already provides further support for the MLB model wherever $\sigma_{\mathrm{e}} = 0$ since all waves should travel at bounded finite speeds and, for a given particle size distribution, γ^∞ is uniformly bounded with respect to Φ. However, the upper bound of ν_N in (6.8) also has a physical meaning. From (3.1), the total solids flux is

(7.2)

$$f^{\mathrm{M}}(\Phi) := \phi_1 v_1 + \cdots + \phi_N v_N = f_1^{\mathrm{M}}(\Phi) + \cdots + f_N^{\mathrm{M}}(\Phi) = \mu V(\phi)(1-\phi)^2 \bar{\varrho}_{\mathrm{s}} \boldsymbol{\delta}^{\mathrm{T}} \Phi.$$

On the other hand, we recall from the definition of $\mathbf{q}$ that

$$v_{\mathrm{f}} = \frac{1}{1-\phi}\big(q - (\phi_1 v_1 + \cdots + \phi_N v_N)\big) = \frac{q - f^{\mathrm{M}}(\Phi)}{1-\phi},$$

where v_{f} is the fluid phase velocity. Since we consider $q = 0$, we obtain $-\mu\bar{\varrho}_{\mathrm{s}} V(\phi)(1-\phi)\boldsymbol{\delta}^{\mathrm{T}}\Phi = v_{\mathrm{f}}$. Thus Lemma 6.1 states that, for relatively dilute suspensions (when $\phi < 1/n$), all eigenvalues (and therefore wave velocities) are bounded by the local velocities of the solid and fluid "particles." In the examples in section 6, we chose $1/n = 0.2128 > \phi_{\mathrm{c}} = 0.2$, such that the model equations are either hyperbolic with the sharp estimates of Lemma 6.1 holding or parabolic.

7.4. Hydrodynamic diffusion. The MLB model (like all other equations for polydisperse suspensions) assumes that $\mathbf{v}_i(\Phi)$ is the velocity of every particle of the ith species at that concentration. Of course, it has long been recognized that identical spheres at the same concentration can have very different velocities. See [111] and [114] for references to early work on this topic. More recently, Segrè, Herbolzheimer, and Chaikin [95] and Guazzelli and colleagues [78, 79, 83] used advanced technology to follow the paths of individual spheres and thereby determine their velocities.

There are essentially three methods of introducing this variability into a model. Historically, the first was the three-parameter Markov model [107, 112], which used the variance and autocorrelation of velocity as additional parameters. A decade later, a model was developed [55] (see also [37]) that combined the variance and autocorrelation in a coefficient of self-induced hydrodynamic diffusion. Thus, the two models are related, but not identical [106]. In both, the parameters must be determined experimentally or computationally. Velocity fluctuations appear to depend on wall effects [111, 114] and density stratification [75, 111] as well as on both the distant [110, 111] and local values of Φ. Theoretical [111], computational [65], and some experimental studies [111] indicate that the variance increases with the size of the container, while other experimental studies [78] show no increase. Recent work by Segrè, Herbolzheimer, and Chaikin [95] and Mucha et al. [75] has gone some way towards resolving this contradiction.

The variability of the velocities of the smaller spheres is considerably increased by the presence of larger or denser spheres [56, 83]. Since the hydrodynamic diffusion

coefficient varies with Φ and $\nabla\Phi$, the diffusion model becomes very complicated [109] for polydisperse suspensions. The Markov model is more tractable [109], but both models require data that are currently lacking. The final method of introducing variability is to use one of several numerical techniques [19, 56, 65]; these solve a specific case and demand considerable computational effort.

Fortunately, the overall behavior of suspensions is usually determined primarily by the mean velocity [84, 113] and does not require the determination of the trajectories of individual spheres [107]. Simulations show that the principal effect of hydrodynamic diffusion is a blurring of the interfaces [19, 108]. In many cases, however, these remain fairly sharp. Experimentally, interfaces are readily detected and, owing to self-sharpening [37, 69], closely approximate discontinuities. Thus, the omission of hydrodynamic diffusion terms at this stage is justified by practical limitations, theoretical considerations, computational comparisons, and experimental results.

7.5. Sediment diffusivity. In the examples discussed in section 6.5, ϕ increases fairly quickly during the consolidation phase, and hence the diffusion of species is highlighted. We recall that the material parameters chosen for the simulations do not correspond to a real suspension; rather, the parameters of the function $\sigma_e(\phi)$ have been chosen such that the numerical simulation produces some clearly visible, distinct effects within a relatively thick sediment layer. The latter point requires that the suspension be highly compressible and therefore that σ_0 and k be relatively large. Thus, strength and rapidity of the diffusion processes are to some extent a consequence of our deliberate choice of parameters, and these effects may be less pronounced for real materials. In fact, it is not clear whether the predicted behavior actually occurs in real suspensions. The assumption that $(\phi_i/\phi)\sigma_e(\phi)$ is that part of σ_e that acts on species i appears to be the obvious choice. Also, (1.2) describes nonlinear diffusion with drift, so it is not surprising that species diffuse to regions of lower concentration.

We mention that nonlinear diffusion in polydisperse suspensions has been considered by Esipov [43] and is postulated as part of a general "competition" mechanism for multispecies granular mixtures by Braun [13]. However, the terms considered in [43] account for hydrodynamic diffusion, and the consequences of the nonlinearity do not appear, since (apparently, for simplicity) these diffusivities are replaced by constants, and cross-diffusivities (e.g., the dependence of the flux of particle species 1 on the flux of species 2) are ignored, while in [13] the nonlinearity is retained, but cross-diffusivities are equally neglected, and no physical interpretation of the origin of nonlinear diffusion is given. In our case, it is difficult to imagine a physical process that leads to the predicted results discussed in section 6.5. In compression, the particles touch each other and support those above. This would appear to make relative movement difficult.

One way out of this dilemma is restricting the movement of particles at very high concentrations. In fact, it has long been held that, at very high concentrations, the particles are locked in place and all species move at the same velocity. This should certainly be true in compressible suspensions. The problem may be not that the diffusion coefficient is much too high in general (which could be fixed, for example, by an appropriate choice of the model functions $V(\phi)$ and $\sigma_e(\phi)$), but that differential diffusion, driven by the gradient $\nabla(\phi_i/\phi)$ in (2.20), becomes dominant when sedimentation is very slow. This is quite unphysical. The first part of the simulations appears reasonable. It is the differential movement at the end that is not.

One way to amend this would be to adopt an idea of Shih, Gidaspow, and Wasan [98], who utilize an expression for the portion of the effective solid stress *gradient*

for each species [98, eq. (10)] that is equivalent to leaving out the term involving $\nabla(\phi_i/\phi)$ in our approach. Unfortunately, the presentation of their numerical solution of a bidisperse system with $\bar{\varrho}_1 = \bar{\varrho}_2$ and $\delta_2 = 0.1766$ is limited to just one profile [98, Figs. 4–6] taken at a time at which the uppermost particles of neither species have reached the sediment layer, a situation that roughly corresponds to $t = 1.5\,\mathrm{h}$ in our Figure 4. However, their solution is similar to ours at that stage, since Figure 4 of [98] shows a concentrated sediment formed by the larger particles with a small portion (actually, only slightly different from the initial concentration) of the smaller. It should be pointed out, of course, that no steady-state prediction of the relative volume fractions ϕ_i/ϕ such as (6.10), (6.11) exists when there are no terms involving that same quantity.

Another way to solve our dilemma, which would go even a step further, would be to change to a common rate of sedimentation at some concentration ϕ^* with $\phi_\mathrm{c} < \phi^* < \phi_\mathrm{max}$. For values of ϕ with $\phi^* < \phi < \phi_\mathrm{max}$, we could eliminate the term in ϕ_i/ϕ in (2.20) and treat the suspension as if all particles were the same size, probably using the average value of δ_i. The best guess for ϕ^* could be found from the simulations by noting the concentrations at which the differential sedimentation dominates. (A possibly more realistic alternative would be to introduce a collective movement gradually, but this would be much more complicated.) Though this solution may seem arbitrary, it does have empirical support. For compressible suspensions, differential sedimentation occurs at medium concentrations. When the concentration is sufficiently high, even dense particles settle at the same speed as the particles of lower density. Thus, the final sediment shows no evidence of segregation; see Been and Sills [5]. When all flocs have the same density, there is a concentration at which initial floc size is unimportant. Essentially, we have a connected structure that is being compressed.

Some more treatments that less closely refer to a particular mathematical model support the similar idea of "en masse" sedimentation of multispecies suspensions at high concentrations [5, 29, 121]. Zeng and Lowe [121] consider rigid-sphere suspensions (not forming compressible sediments) but postulate the existence of a "critical concentration," in the sense of the quantity ϕ^* (*not* ϕ_c) introduced above, at which change in sedimentation behavior from differential settling (size fractionation) to "en-masse settling of the entire suspension" occurs [121], and they indicate that values of ϕ^* ranging from 0.3 to 0.55 are suitable, depending on the material. Related experimental findings were reported much earlier by Shannon and coworkers [96, 97], who observed that for equal-density spheres (normally distributed in diameters plus a tail of fines), the rise of the packed bed showed that the solids flux remained constant throughout (in contrast to sedimentation of dilute suspensions, in which the flux decreases after the larger particles have settled out).

The previous discussion shows that there is no obvious unique way to reduce the sediment diffusivity seen in our numerical examples. Published experimental information to which the numerical predictions could be compared is scarce (see the references cited in this section and [9, 116]), and a definite solution of the problems discussed here cannot be suggested. Basically, there seem to exist three alternatives.

Our approach is based on a rigorous derivation and establishes a polydisperse sedimentation model that is "well-posed" in the sense that strict parabolicity is about the best property we can expect system (1.2) to have whenever the right-hand part is different from zero (i.e., for $\phi_\mathrm{c} < \phi < \phi_\mathrm{max}$). This property, combined with the hyperbolicity of the first-order system, makes the model amenable to numerical so-

lution and is conserved when we vary the model functions $V(\phi)$ and $\sigma_e(\phi)$ to reduce sediment diffusivity. In the monodisperse case, it turned out that using the expression $V(\phi) = (1-\phi)^{n-2}$ for all ranges of concentration values (as, for simplicity, done here) leads to an overestimation of particle diffusivity in the sediment, and better agreement was obtained by using piecewise definition of $V(\phi)$ or of the resulting flux density function $f^M(\phi)$; see [15, 16]. The emphasis here is on a *gradual* variation of the parameters, which leaves the nature of the model unaltered.

The next step of modification would be "switching off" the term $\nabla(\phi_i/\phi)$ in (2.20) on the interval $[\phi^*, \phi_{\max}]$, where we admit the limiting case $\phi^* = \phi_c$. The mathematical consequences of such a reduction can be derived easily, since in the derivation of section 4, $\sigma_e(\phi)$ and its derivative $\sigma_e'(\phi)$ are formally treated as independent functions. Thus for the parabolicity analysis, deleting $\nabla(\phi_i/\phi)$ in (2.20) corresponds to sending σ_e to zero and leaving the occurrences of $\sigma_e'(\phi)$ unchanged. From (4.1) we see that then $\mathbf{A}(\Phi)$ is a rank-one matrix having $N-1$ eigenvalues that vanish. The system is then no longer strictly parabolic for $\phi \in [\phi^*, \phi_{\max}]$. This case is explicitly excluded in the analysis of certain schemes [68] but is admitted in others [60] and still has the advantage that explicit tracking of the sediment-suspension interface is unnecessary.

The most radical modification would be to change to an "en masse" sedimentation model for $\phi \in [\phi^*, \phi_{\max}]$. In particular, this would imply that $\phi = \phi^*$ denotes an interface across which we change from the system of N convection-diffusion equations (1.2) to one scalar equation, i.e., between two different models. This idea is viable when we a priori do not wish to differentiate between size classes in the sediment. In fact, this is the main idea of the model advanced by Stamatakis and Tien [102]. There is an advantage in computation time when there is a region in which a scalar equation instead of an $N \times N$ system has to be solved, but formulating transition conditions across the model change interface and tracking it during computation may become complicated.

7.6. Applications. Been and Sills [5] measured local changes in particle size distribution due to the relative movement of particles of different sizes under the influence of effective solid stress and at different initial concentrations. Their experiments were performed with estuarine mud, a natural mixture composed of many different materials for which the constitutive model equations are difficult to determine. More precise knowledge of these functions can be expected in chemical engineering applications, where the settling solids are usually formed by a product having more homogeneous material properties. The model outlined herein should thus be useful for simulations in any of the industrial applications cited in section 1. In particular, the model can also be applied to centrifugal configurations and pressure filtration (see [15, 21] for the monodisperse cases) and thereby be employed to simulate the manufacturing and final composition of ceramic materials with functionally graded material properties (see [9, 10, 11]). Comparing our Figures 2 and 3 illustrates that the effective stress is a decisive factor when the variation of sediment composition should be continuous.

Acknowledgments. We thank the referees for valuable comments and suggestions.

REFERENCES

[1] H. Arastoopour, S.C. Lin, and S.A. Weil, *Analysis of vertical pneumatic conveying of solids using multiphase flow models*, AIChE J., 28 (1982), pp. 467–473.

[2] D. Aregba-Driollet, R. Natalini, and S. Tang, *Diffusive Kinetic Explicit Schemes for*

Nonlinear Degenerate Parabolic Systems, preprint, Norwegian University of Science and Technology Conservation Laws Preprint Server, Tondheim, Norway, 2000; available online at http://www.math.ntnu.no/conservation/.

[3] L.G. Austin, C.H. Lee, and F. Concha, *Hindered settling and classification partition curves*, Minerals & Metallurgical Process., 9 (1992), pp. 161–168.

[4] G.K. Batchelor and R.W. Janse van Rensburg, *Structure formation in bidisperse sedimentation*, J. Fluid Mech., 166 (1986), pp. 370–407.

[5] K. Been and G.C. Sills, *Self-weight consolidation of soft soils: An experimental and theoretical study*, Géotechnique, 31 (1981), pp. 519–535.

[6] P. Bénilan and H. Touré, *Sur l'équation générale* $u_t = \varphi(u)_{xx} - \psi(u)_x + v$, C. R. Acad. Sci. Paris Sér. I Math., 299 (1984), pp. 919–922.

[7] P. Bénilan and H. Touré, *Sur l'équation générale* $u_t = a(\cdot, u, \phi(\cdot, u)_x)_x + v$ *dans* L^1. I. *Étude du problème stationnaire*, in Evolution Equations, Proceedings of the International Conference Held at Louisiana State University (Baton Rouge, LA, 1992), G. Ferreyra, G. Ruiz Goldstein, and F. Neubrander, eds., Marcel Dekker, New York, 1995, pp. 35–62.

[8] P. Bénilan and H. Touré, *Sur l'équation générale* $u_t = a(\cdot, u, \phi(\cdot, u)_x)_x + v$ *dans* L^1. II. *Le problème d'évolution*, Ann. Inst. H. Poincaré Anal. Non Linéaire, 12 (1995), pp. 727–761.

[9] P.M. Biesheuvel, *Particle segregation during pressure filtration for cast formation*, Chem. Engrg. Sci., 55 (2000), pp. 2595–2606.

[10] P.M. Biesheuvel and H. Verweij, *Calculation of the composition profile of a functionally graded material by centrifugal casting*, J. Amer. Ceram. Soc., 83 (2000), pp. 743–749.

[11] P.M. Biesheuvel, V. Breedveld, A.P. Higler, and H. Verweij, *Graded membrane supports produced by centrifugal casting of a slightly polydisperse suspension*, Chem. Engrg. Sci., 56 (2001), pp. 3517–3525.

[12] F. Bouchut, F.R. Guarguaglini, and R. Natalini, *Diffusive BGK approximations for nonlinear multidimensional parabolic equations*, Indiana Univ. Math. J., 49 (2000), pp. 723–749.

[13] J. Braun, *Segregation of granular media by diffusion and convection*, Phys. Rev. E, 64 (2001), paper 011307.

[14] R. Bürger, F. Concha, K.-K. Fjelde, and K.H. Karlsen, *Numerical simulation of the settling of polydisperse suspensions of spheres*, Powder Technol., 113 (2000), pp. 30–54.

[15] R. Bürger, F. Concha, and K.H. Karlsen, *Phenomenological model of filtration processes:* 1. *Cake formation and expression*, Chem. Engrg. Sci., 56 (2001), pp. 4537–4553.

[16] R. Bürger, F. Concha, and F.M. Tiller, *Applications of the phenomenological theory to several published experimental cases of sedimentation processes*, Chem. Engrg. J., 80 (2000), pp. 105–117.

[17] R. Bürger, S. Evje, and K.H. Karlsen, *On strongly degenerate convection-diffusion problems modeling sedimentation-consolidation processes*, J. Math. Anal. Appl., 247 (2000), pp. 517–556.

[18] R. Bürger, S. Evje, K. H. Karlsen, and K.-A. Lie, *Numerical methods for the simulation of the settling of flocculated suspensions*, Chem. Engrg. J., 80 (2000), pp. 91–104.

[19] R. Bürger, K.-K. Fjelde, K. Höfler, and K.H. Karlsen, *Central difference solutions of the kinematic model of settling of polydisperse suspensions and three-dimensional particle-scale simulations*, J. Engrg. Math., 41 (2001), pp. 167–187.

[20] R. Bürger and K.H. Karlsen, *On some upwind difference schemes for the phenomenological sedimentation-consolidation model*, J. Engrg. Math., 41 (2001), pp. 145–166.

[21] R. Bürger and K.H. Karlsen, *A strongly degenerate convection-diffusion problem modeling centrifugation of flocculated suspensions*, in Hyperbolic Problems: Theory, Numerics, Applications (Proceedings of the Eighth International Conference, Magdeburg, Germany, 2000), Vol I, H. Freistühler and G. Warnecke, eds., Internat. Ser. Numer. Math. 140, Birkhäuser-Verlag, Basel, 2001, pp. 207–216.

[22] R. Bürger, K.H. Karlsen, E.M. Tory, and W.L. Wendland, *Model equations and instability regions for the sedimentation of polydisperse suspensions of spheres*, Z. Angew. Math. Mech., 82 (2002), pp. 699–722.

[23] R. Bürger and M. Kunik, *A critical look at the kinematic-wave theory for sedimentation-consolidation processes in closed vessels*, Math. Methods Appl. Sci., 24 (2001), pp. 1257–1273.

[24] R. Bürger, C. Liu, and W.L. Wendland, *Existence and stability for mathematical models of sedimentation-consolidation processes in several space dimensions*, J. Math. Anal. Appl., 264 (2001), pp. 288–310.

[25] R. Bürger and W. L. Wendland, *Existence, uniqueness, and stability of generalized solu-*

tions of an initial-boundary value problem for a degenerating quasilinear parabolic equation, J. Math. Anal. Appl., 218 (1998), pp. 207–239.

[26] R. Bürger, W.L. Wendland, and F. Concha, *Model equations for gravitational sedimentation-consolidation processes*, Z. Angew. Math. Mech., 80 (2000), pp. 79–92.

[27] M.C. Bustos, F. Concha, R. Bürger, and E.M. Tory, *Sedimentation and Thickening*, Kluwer Academic Publishers, Dordrecht, The Netherlands, 1999.

[28] J. Carrillo, *Entropy solutions for nonlinear degenerate problems*, Arch. Ration. Mech. Anal., 147 (1999), pp. 269–361.

[29] J.C. Chang, B.V. Velakamanni, F.F. Lange, and D.S. Pearson, *Centrifugal consolidation of Al_2O_3 and Al_2O_3/ZrO_2 composite slurries vs. interparticle potentials: Particle packing and mass segregation*, J. Amer. Ceram. Soc., 74 (1991), pp. 2201–2204.

[30] G.-Q. Chen and E. DiBenedetto, *Stability of entropy solutions to the Cauchy problem for a class of nonlinear hyperbolic-parabolic equations*, SIAM J. Math. Anal., 33 (2001), pp. 751–762.

[31] G.-Q. Chen and B. Perthame, *Well-posedness for anisotropic degenerate parabolic-hyperbolic equations*, Ann. Inst. H. Poincaré Anal. Nonlinéaire, 20 (2003), pp. 645–668.

[32] G.-Q. Chen and D. Wang, *The Cauchy problem for the Euler equations for compressible fluids*, in Handbook of Mathematical Fluid Dynamics, Vol. 1, S.J. Friedlander and D. Serre, eds., Elsevier Science, Amsterdam, 2002, pp. 421–543.

[33] B. Cockburn and C.-W. Shu, *The local discontinuous Galerkin method for time-dependent convection-diffusion systems*, SIAM J. Numer. Anal., 35 (1998), pp. 2440–2463.

[34] F. Concha and M.C. Bustos, *Theory of sedimentation of flocculated fine particles*, in Flocculation, Sedimentation and Consolidation, B.M. Moudgil and P. Somasundaran, eds., American Institute of Chemical Engineers, New York, 1986, pp. 275–284.

[35] F. Concha, M.C. Bustos, and A. Barrientos, *Phenomenological theory of sedimentation*, in Sedimentation of Small Particles in a Viscous Fluid, E.M. Tory, ed., Computational Mechanics Publications, Southampton, UK, 1996, pp. 51–96.

[36] P. D'Ancona and S. Spagnolo, *The Cauchy problem for weakly parabolic systems*, Math. Ann., 309 (1997), pp. 307–330.

[37] R.H. Davis, *Hydrodynamic diffusion of suspended particles: A symposium*, J. Fluid Mech., 310 (1996), pp. 325–335.

[38] R.H. Davis and H. Gecol, *Hindered settling function with no empirical parameters for polydisperse suspensions*, AIChE J., 40 (1994), pp. 570–575.

[39] R. De Boer, *Theory of Porous Media*, Springer-Verlag, Berlin, 2000.

[40] P. Diplas and A.N. Papanicolaou, *Batch analysis of slurries in zone settling regime*, J. Environ. Engrg., 123 (1999), pp. 659–667.

[41] D.A. Drew and L.A. Segel, *Averaged equations for two-phase flows*, Stud. Appl. Math., 50 (1971), pp. 205–231.

[42] S.D. Eidel'man, *Parabolic Systems*, North-Holland, Amsterdam, London, 1969.

[43] S.E. Esipov, *Coupled Burgers equations: A model of polydispersive sedimentation*, Phys. Rev. E, 52 (1985), pp. 3711–3718.

[44] M.S. Espedal and K.H. Karlsen, *Numerical solution of reservoir flow models based on large time step operator splitting algorithms*, in Filtration in Porous Media and Industrial Applications, Lecture Notes of the C.I.M.E course (Cetraro, Italy, 1998), A. Fasano, ed., Lecture Notes in Math. 1734, Springer-Verlag, Berlin, 2000, pp. 9–77.

[45] S. Evje and K.H. Karlsen, *Monotone difference approximations of BV solutions to degenerate convection-diffusion equations*, SIAM J. Numer. Anal., 37 (2000), pp. 1838–1860.

[46] R. Eymard, T. Gallouët, R. Herbin, and A. Michel, *Convergence of a finite volume scheme for nonlinear degenerate parabolic equations*, Numer. Math., 92 (2002), pp. 41–82.

[47] A. Fitt, *Mixed systems of conservation laws in industrial mathematical modelling*, Surveys Math. Indust., 6 (1996), pp. 21–53.

[48] X. Flotats, *Mathematical modeling of polydisperse suspensions sedimentation*, Hungarian J. Indust. Chem., 23 (1995), pp. 215–221.

[49] A. Friedman, *Partial Differential Equations of Parabolic Type*, Prentice–Hall, Englewood Cliffs, NJ, 1964.

[50] D. Gidaspow, *Multiphase Flow and Fluidization*, Academic Press, San Diego, 1994.

[51] E. Godlewski and P.-A. Raviart, *Numerical Approximation of Hyperbolic Systems of Conservation Laws*, Springer-Verlag, New York, 1996.

[52] M.D. Green, M. Eberl, and K.A. Landman, *Compressive yield stress of flocculated suspensions: Determination via experiment*, AIChE J., 42 (1996), pp. 2308–2318.

[53] M. Gurtin, *An Introduction to Continuum Mechanics*, Acadamic Press, San Diego, 1981.
[54] K. Gustavsson, J. Oppelstrup, and J. Eiken, *Consolidation of concentrated suspensions—Shear and irreversible floc structure rearrangement*, Comput. Visual. Sci., 4 (2001), pp. 61–66.
[55] J.M. Ham and G.M. Homsy, *Hindered settling and hydrodynamic dispersion in quiescent sedimenting suspensions*, Int. J. Multiphase Flow, 14 (1988), pp. 533–546.
[56] K. Höfler, *Simulation and Modeling of Mono- and Bidisperse Suspensions*, Doctoral thesis, Institute for Computer Applications 1, University of Stuttgart, Stuttgart, Germany, 2000.
[57] H. Holden, K.H. Karlsen, and N.H. Risebro, *On uniqueness and existence of entropy solutions of weakly coupled systems of nonlinear degenerate parabolic equations*, Electron. J. Differential Equations, No. 46 (2003), pp. 1–31.
[58] F. Hubert, *Global existence for hyperbolic-parabolic systems with large periodic initial data*, Differential Integral Equations, 11 (1998), pp. 69–83.
[59] B.L. Keyfitz, *Multiphase saturation equations, change of type and inaccessible regions*, in Flow in Porous Media, J. Douglas and U. Hornung, eds., Birkhäuser-Verlag, Basel, Boston, Berlin 1993, pp. 103–116.
[60] K.H. Karlsen, K.-A. Lie, J.R. Natvig, H.F. Nordhaug, and H.K. Dahle, *Operator splitting methods for systems of convection-diffusion equations: Nonlinear error mechanisms and correction strategies*, J. Comput. Phys., 173 (2001), pp. 636–663.
[61] K.H. Karlsen and M. Ohlberger, *A note on the uniqueness of entropy solutions of nonlinear degenerate parabolic equations*, J. Math. Anal. Appl., 275 (2002), pp. 439–458.
[62] K.H. Karlsen and N.H. Risebro, *On the uniqueness and stability of entropy solutions of nonlinear degenerate parabolic equations with rough coefficients*, Discrete Contin. Dyn. Syst. Ser. A, 9 (2003), pp. 1081–1104.
[63] H.-O. Kreiss and J. Lorenz, *Initial-Boundary Value Problems and the Navier–Stokes Equations*, Academic Press, Boston, MA, 1989.
[64] A. Kurganov and E. Tadmor, *New high-resolution central schemes for nonlinear conservation laws and convection-diffusion equations*, J. Comput. Phys., 160 (2000), pp. 241–282.
[65] A.J.C. Ladd, *Sedimentation of homogeneous suspensions of non-Brownian spheres*, Phys. Fluids, 9 (1997), pp. 491–499.
[66] O.A. Ladyženskaja, V.A. Solonnikov, and N.N. Ural'ceva, *Linear and Quasilinear Equations of Parabolic Type*, AMS Trans. Math. Monogr. 23, AMS, Providence, RI, 1968.
[67] K.A. Landman and L.R. White, *Solid/liquid separation of flocculated suspensions*, Adv. Colloid Interface Sci., 51 (1994), pp. 175–246.
[68] C. Lattanzio and R. Natalini, *Convergence of diffusive BGK approximations for nonlinear strongly parabolic systems*, Proc. Roy. Soc. Edinburgh Sect. A, 132 (2002), pp. 341–358.
[69] S. Lee, Y. Jang, C. Choi, and T. Lee, *Combined effect of sedimentation velocity fluctuation and self-sharpening on interface broadening*, Phys. Fluids A, 4 (1992), pp. 2601–2606.
[70] I-S. Liu, *Continuum Mechanics*, Springer-Verlag, Berlin, 2002.
[71] M.J. Lockett and K.S. Bassoon, *Sedimentation of binary particle mixtures*, Powder Technol., 24 (1979), pp. 1–7.
[72] C. Mascia, A. Porretta, and A. Terracina, *Non-homogeneous Dirichlet problems for degenerate parabolic-hyperbolic equations*, Arch. Ration. Mech. Anal., 163 (2002), pp. 87–124.
[73] J.H. Masliyah, *Hindered settling in a multiple-species particle system*, Chem. Engrg. Sci., 34 (1979), pp. 1166–1168.
[74] M. Massoudi, K.R. Rajagopal, J.M. Ekmann, and M.P. Mathur, *Remarks on the modeling of fluidized systems*, AIChE J., 38 (1992), pp. 471–472.
[75] P.J. Mucha, S.-Y. Tee, D.A. Weitz, B.I. Shraiman, and M.P. Brenner, *A unifying theory for velocity fluctuations in sedimentation*, J. Fluid Mech., submitted.
[76] K. Nakamura and C.E. Capes, *Vertical pneumatic conveying of binary particle mixtures*, in Fluidization Technology, Vol. 2, D.L. Keairns, ed., Hemisphere Publishing, Washington, DC, 1976, pp. 159–184.
[77] H. Nessyahu and E. Tadmor, *Non-oscillatory central differencing for hyperbolic conservation laws*, J. Comput. Phys., 87 (1990), pp. 408–463.
[78] H. Nicolai and E. Guazzelli, *Effect of vessel size on the hydrodynamic diffusion of sedimenting spheres*, Phys. Fluids, 7 (1995), pp. 3–5.
[79] H. Nicolai, B. Herzhaft, E.J. Hinch, L. Oger, and E. Guazzelli, *Particle velocity fluctuations and hydrodynamic self-diffusion of sedimenting non-Brownian spheres*, Phys. Fluids, 8 (1995), pp. 12–23.
[80] M. Ohlberger, *A posteriori error estimates for vertex centered finite volume approxima-*

tions of convection-diffusion-reaction equations, Math. Model. Numer. Anal., 35 (2001), pp. 355–387.

[81] V. Pane and R.L. Schiffman, *A note on sedimentation and consolidation*, Géotechnique, 35 (1985), pp. 69–72.

[82] S.L. Passman and D.A. Drew, *A simple multicomponent fluid theory with accurate physics*, in Recent Developments in Structured Continua, D. De Kee and P.N. Kaloni, eds., Pitman Res. Notes Math. 229, Harlow, UK, 1990, pp. 293–300.

[83] Y. Peysson and E. Guazzelli, *Velocity fluctuations in a bidisperse sedimenting suspension*, Phys. Fluids, 11 (1999), pp. 1953–1955.

[84] D.K. Pickard and E.M. Tory, *Experimental implications of a Markov model for sedimentation*, J. Math. Anal. Appl., 72 (1979), pp. 150–176.

[85] M. Renardy, *A degenerate parabolic-hyperbolic system modeling the spreading of surfactants*, SIAM J. Math. Anal., 28 (1997), pp. 1048–1063.

[86] J.F. Richardson and W.N. Zaki, *Sedimentation and fluidization: Part* I, Trans. Inst. Chem. Engrs. (London), 32 (1954), pp. 35–53.

[87] F. Rosso and G. Sona, *Gravity-driven separation of oil-water dispersions*, Adv. Math. Sci. Appl., 11 (2001), pp. 127–151.

[88] A. Rushton, A.S. Ward, and R.G. Holdich, *Solid-Liquid Filtration and Sedimentation Technology*, 2nd ed., Wiley-VCH, Weinheim, Germany, 2000.

[89] W.K. Sartory, *Three-component analysis of blood sedimentation by the method of characteristics*, Math. Biosci., 33 (1977), pp. 145–165.

[90] U. Schaflinger, *Enhanced centrifugal separation with finite Rossby numbers in cylinders with compartment-walls*, Chem. Engrg. Sci., 42 (1987), pp. 1197–1205.

[91] U. Schaflinger, A. Köppl, and G. Filipczak, *Sedimentation in cylindrical centrifuges with compartments*, Ingenieur-Archiv, 56 (1986), pp. 321–331.

[92] R.L. Schiffman, V. Pane, and R.E. Gibson, *The theory of one-dimensional consolidation of saturated clays:* IV. *An overview of nonlinear finite strain sedimentation and consolidation*, in Sedimentation-Consolidation Models: Predictions and Validations, R.N. Yong and F.C. Townsend, eds., American Society of Civil Engineers, New York, 1984, pp. 1–29.

[93] W. Schneider, *Kinematic-wave theory of sedimentation beneath inclined walls*, J. Fluid Mech., 120 (1982), pp. 323–346.

[94] W. Schneider, G. Anestis, and U. Schaflinger, *Sediment composition due to settling of particles of different sizes*, Int. J. Multiphase Flow, 11 (1985), pp. 419–423.

[95] P.N. Segrè, E. Herbolzheimer, and P.M. Chaikin, *Long-range correlations in sedimentation*, Phys. Rev. Lett., 79 (1997), pp. 2574–2577.

[96] P.T. Shannon, R.D. DeHaas, E.P. Stroupe, and E.M. Tory, *Batch and continuous thickening*, Industrial and Engineering Chemistry Fundamentals, 3 (1964), pp. 250–260.

[97] P.T. Shannon, E.P. Stroupe, and E.M. Tory, *Batch and continuous thickening*, Industrial and Engineering Chemistry Fundamentals, 2 (1963), pp. 203–211.

[98] Y.T. Shih, D. Gidaspow, and D.T. Wasan, *Hydrodynamics of sedimentation of multisized particles*, Powder Technol., 50 (1987), pp. 201–215.

[99] G.F. Smith, *On isotropic functions of symmetric tensors, skew-symmetric tensors and vectors*, Int. J. Engrg. Sci., 9 (1971), pp. 899–916.

[100] J. Smoller, *Shock Waves and Reaction-Diffusion Equations*, 2nd ed., Springer-Verlag, New York, 1994.

[101] A. Spannenberg and K.P. Galvin, *Continuous differential sedimentation of a binary suspension*, Chem. Engrg. in Australia, 21 (1996), pp. 7–11.

[102] K. Stamatakis and C. Tien, *Batch sedimentation calculations—The effect of compressible sediment*, Powder Technol., 72 (1992), pp. 227–240.

[103] E. Tadmor, *Approximate solutions of nonlinear conservation laws*, in Advanced Numerical Approximation of Nonlinear Hyperbolic Equations, B. Cockburn, C. Johnson, C.-W. Shu, and E. Tadmor, eds., Lecture Notes in Math. 1697, Springer-Verlag, Berlin, 1998, pp. 1–149.

[104] M.E. Taylor, *Partial Differential Equations* III, Springer-Verlag, New York, 1996.

[105] F.M. Tiller, R. Lu, J.H. Kwon, and D.J. Lee, *Variable flow rate in compactible filter cakes*, Water Res., 33 (1999), pp. 15–22.

[106] E.M. Tory, *Stochastic sedimentation and hydrodynamic diffusion*, Chem. Engrg. J., 80 (2000), pp. 81–89.

[107] E.M. Tory, M. Bargieł, and R.L. Honeycutt, *A three-parameter Markov model for sedimentation* III. *A stochastic Runge–Kutta method for computing first-passage times*, Powder Technol., 80 (1994), pp. 133–146.

[108] E.M. Tory and R.A. Ford, *Simulation of sedimentation of bidisperse suspensions*, Int. J.

Mineral Process., to appear.

[109] E.M. Tory and R.A. Ford, *Simulation of sedimentation of monodisperse and polydisperse suspensions*, in Analysis and Simulation of Multifield Problems, W. Wendland and M. Efendiev, eds., Springer-Verlag, Berlin, 2003, pp. 343–348.

[110] E.M. Tory and M.T. Kamel, *On the divergence problem in calculating particle velocities in dilute suspensions of identical spheres* II. *Effect of a plane wall*, Powder Technol., 55 (1988), pp. 51–59; *Erratum*, Powder Technol., 94 (1997), p. 265.

[111] E.M. Tory, M.T. Kamel, and C.F. Chan Man Fong, *Sedimentation is container-size dependent*, Powder Technol., 73 (1992), pp. 219–238.

[112] E.M. Tory and D.K. Pickard, *A three-parameter Markov model for sedimentation*, Can. J. Chem. Engrg., 55 (1977), pp. 655–665.

[113] E.M. Tory and D.K. Pickard, *Extensions and refinements of a Markov model for sedimentation*, J. Math. Anal. Appl., 86 (1982), pp. 442–470.

[114] E.M. Tory and D.K. Pickard, *Experimental evidence for a stochastic approach to sedimentation*, in Flocculation, Sedimentation and Consolidation, B.M. Moudgil and P. Somasundaran, eds., American Institute of Chemical Engineers, New York, 1986, pp. 297–306.

[115] C.-C. Wang, *A new representation theorem for isotropic functions: An answer to Professor G.F. Smith's criticism of my papers on representations for isotropic functions*. I. *Scalar-valued isotropic functions*, Arch. Ration. Mech. Anal., 36 (1970), pp. 166–197.

[115A] C.-C. Wang, *A new representation theorem for isotropic functions: An answer to Professor G.F. Smith's criticism of my papers on representations for isotropic functions*. II. *Vector-valued isotropic functions, symmetric tensor-valued isotropic functions, and skew-symmetric tensor-valued isotropic functions*, Arch. Ration. Mech. Anal., 36 (1970), pp. 198–223.

[115B] C.-C. Wang, *Corrigendum to my recent papers on "Representations for isotropic functions,"* Arch. Ration. Mech. Anal., 43 (1971), pp. 392–395.

[116] D.J. Wedlock, I.J. Fabris, and J. Grimsey, *Sedimentation in polydisperse particulate suspensions*, Colloids and Surfaces, 43 (1990), pp. 67–81.

[117] R.H. Weiland, Y.P. Fessas, and B.V. Ramarao, *On instabilities arising during sedimentation of two-component mixtures of solids*, J. Fluid Mech., 142 (1984), pp. 383–389.

[118] A.I. Vol'pert and S.I. Hudjaev, *Cauchy's problem for degenerate second order quasilinear parabolic equations*, Math. USSR Sb., 7 (1969), pp. 365–387.

[119] Z. Wu and J. Yin, *Some properties of functions in BV_x and their applications to the uniqueness of solutions for degenerate quasilinear parabolic equations*, Northeastern Math. J., 5 (1989), pp. 395–422.

[120] Z. Wu, J. Zhao, J. Yin, and H. Li, *Nonlinear Diffusion Equations*, World Scientific, Singapore, 2001.

[121] J. Zeng and D.R. Lowe, *A numerical model for sedimentation from highly-concentrated multi-sized suspensions*, Math. Geol., 24 (1992), pp. 393–415.

[122] Y. Zimmels, *Theory of density separation of particulate systems*, Powder Technol., 43 (1985), pp. 127–139.